Systematics and Biodiversity

ISSN: (Print) (Online) Journal homepage: www.tandfonline.com/journals/tsab20

Integrative taxonomy of *Tethya*: description of four new species based on morphology, phylogeny and microbiome diversity

Nadia Santodomingo, Cristina Díez-Vives, Nathan J. Kenny, Paco Cárdenas, Laura Balcells, Juan Moles, Sven Zea, Gonzalo Giribet, Emilio Lanna, Carlota Gracia-Sancha & Ana Riesgo

To cite this article: Nadia Santodomingo, Cristina Díez-Vives, Nathan J. Kenny, Paco Cárdenas, Laura Balcells, Juan Moles, Sven Zea, Gonzalo Giribet, Emilio Lanna, Carlota Gracia-Sancha & Ana Riesgo (2024) Integrative taxonomy of *Tethya*: description of four new species based on morphology, phylogeny and microbiome diversity, Systematics and Biodiversity, 22:1, 2383341, DOI: 10.1080/14772000.2024.2383341

To link to this article: https://doi.org/10.1080/14772000.2024.2383341

Systematics and Biodiversity (2024), **22(1)**: 2383341

Taylor & Francis
Taylor & Francis Group

Research Article

Integrative taxonomy of *Tethya*: description of four new species based on morphology, phylogeny and microbiome diversity

NADIA SANTODOMINGO[1,2], CRISTINA DÍEZ-VIVES[1,3], NATHAN J. KENNY[1,4], PACO CÁRDENAS[5], LAURA BALCELLS[6], JUAN MOLES[7], SVEN ZEA[8], GONZALO GIRIBET[9], EMILIO LANNA[10], CARLOTA GRACIA-SANCHA[11] & ANA RIESGO[1,11]

[1]Department of Life Sciences, The Natural History Museum, London SW7 5BD, UK
[2]Department of Earth Sciences, University of Oxford, S. Parks Road, Oxford OX1 3AN, UK
[3]Department of Systems Biology, Centro Nacional de Biotecnología, c/Darwin, 3, Madrid 28049, Spain
[4]Department of Biochemistry, University of Otago, PO Box 56, Dunedin, Aotearoa 9054, New Zealand
[5]Museum of Evolution, Uppsala University, Norbyvägen 16, Uppsala 752 36, Sweden
[6]NatureMetrics, 1 Occam Court, Surrey Research Park, Guildford GU2 7HJ, UK
[7]Institut de Recerca de la Biodiversitat (IRBio) & Departament de Biologia Evolutiva, Ecologia i Ciències Ambientals, Facultat de Biologia, Av. Diagonal 643, Barcelona 08028, Spain
[8]Universidad Nacional de Colombia, Sede Caribe, Instituto de Estudios en Ciencias del Mar (CECIMAR), c/o INVEMAR, Calle 25 2-55, Playa Salguero – Rodadero Sur, Santa Marta 40006, Colombia
[9]Department of Organismic and Evolutionary Biology, Harvard University, 26 Oxford Street, Cambridge, MA, USA
[10]Instituto de Biologia, Universidade Federal da Bahia, Rua Barão de Jeremoabo, s/n, Campus Ondina, Salvador 40170-115, Brazil Bahia
[11]Department of Biodiversity and Evolutionary Biology, Museo Nacional de Ciencias Naturales (CSIC), c/José Gutiérrez Abascal 2, Madrid 28006, Spain

(Received 5 July 2024; accepted 8 July 2024)

The genus *Tethya*, one of the most iconic groups in the phylum Porifera. includes nearly 100 valid species. *Tethya* shows a nearly cosmopolitan distribution, and thus this clade could help elucidate global mechanisms of speciation in sponges. Contrasting with many other marine organisms, *Tethya* peaks in diversity in the temperate region, with only ∼30% of diversity occurring in the tropics. This pattern may however be related to a lack of studies in the tropics, masked by dubious taxonomic identifications. To address this question, we studied new collections from the Western Atlantic (Caribbean and Brazil) and the Northeastern Atlantic, as well as museum material from the Indian Ocean. Combining morphological investigation with molecular phylogenetics and the study of the sponge's microbial communities, we conclude that four constitute new species that we describe here: *Tethya martini* Riesgo, Giribet, & Santodomingo, sp. nov.; *Tethya simoni* Santodomingo, Zea, & Riesgo, sp. nov.; *Tethya erici* Díez-Vives, Santodomingo, Moles, & Riesgo, sp. nov.; *Tethya orioni* Kenny, Santodomingo & Riesgo, sp. nov. Some species thought to be widespread (e.g., *T. aurantium* and *T. seychellensis*), each represent multiple species with unique geographic distributions. A phylogenetic analysis of *Tethya* (based on COI and 28S rRNA sequence data) recovered five main clades, which were also characterized by distinct prokaryotic communities. This suggests that microbiomes could be used as a guide for taxonomic identification in *Tethya*. We finally explored the existence of a phylosymbiotic pattern in sponges at different levels of prokaryotic taxonomic resolution (i.e., at phylum, class, and genus-level analysis of prokaryotes). Remarkably, our analysis revealed high levels of coevolution of *Tethya* and their associated microbial communities, even when microbiomes were analysed at the genus level. Our findings support the use of an integrative approach to better understand the evolutionary history of sponges.

http://zoobank.org/urn:lsid:zoobank.org:pub:54F80E5E-99A4-43CE-BA3A-BCD01E715595

Key words: systematics, microbiome, spicules, sponges, phylogeny

Correspondence to: Nadia Santodomingo E-mail: n.santodomingo@nhm.ac.uk; Ana Riesgo E-mail: anariesgogil@mncn.csic.es

ISSN 1477-2000 print / 1478-0933 online

https://dx.doi.org/10.1080/14772000.2024.2383341
Published online 14 Oct 2024

Introduction

Sponges in the genus *Tethya* Lamarck, 1815 are iconic taxa among the phylum Porifera (Sarà, 2002) for being the only metazoans with spherical symmetry (Brusca et al., 2023). Their spherical shape, well-defined cortex, and surface usually covered by tubercles and buds, are characteristics that give *Tethya* the common name of 'golf balls', and make this genus one of the most easily recognized groups of species among demosponges (Sarà, 1987). There have been 96 accepted species described worldwide since the original designation of the genus name *Tethya* by Lamarck in 1815 (de Voogd et al., 2024). They have been noted to occur from shallow coastal waters to the deep sea, in all oceans except the poles (Bergquist & Kelly-Borges, 1991; Sarà, 2002).

Some of the first species described for the genus, *Tethya aurantium* (Pallas, 1766), *T. seychellensis* (Wright, 1881), *T. diploderma* Schmidt, 1870, and *T. japonica* Sollas, 1888, were long thought to be cosmopolitan or having a broad distribution range (Sarà, 1987). However, some records remained dubious and were later confirmed to belong to undescribed species (Bergquist & Kelly-Borges, 1991; Ribeiro & Muricy, 2004, 2011). Regional inventories conducted over the past 30 years have uncovered a hidden diversity of *Tethya*, with species described from Australia and New Zealand (Bergquist & Kelly-Borges, 1991; Sarà & Sarà, 2004), Brazil (Ribeiro & Muricy, 2004, 2011), the Mexican Pacific and California (Austin et al., 2014; Sarà Gómez, & Sarà, 2001), as well as Galápagos (Desqueyroux-Fáundez & van Soest, 1997; Sarà et al., 2000; Sim-Smith et al., 2021). The remaining described *Tethya* species are thought to be widely distributed across the Mediterranean Sea, the North Atlantic Ocean, North Pacific Ocean, with a few species described in the Chilean fjords, the Caribbean Sea, and the Indian Ocean. From all this diversity, over 60% of the *Tethya* species occur in temperate waters, about 30% are from the tropics, and 10% have a widespread distribution in both temperate and tropical waters. Although the current *Tethya* distribution could be a result of an underlying biogeographic pattern, it could also be attributed to a collection bias, as in other poriferan groups (van Soest et al., 2012) and lack of studies in the tropical region, in particular the central Indo-Pacific and the Caribbean. To date, only six species are known from the Caribbean: the imprecise type locality of *T. diploderma* and *T. globum* Duchassaing de Fonbressin & Michelotti, 1864 is Antilles; *Tethya actinia* de Laubenfels & Hindle, 1950 was first described from Bermuda; and *T. maza* Selenka, 1879 was described from southern Brazil. The other two Caribbean species, *T. aurantium* and *T. seychellensis*, have type localities in the Mediterranean Sea and the Seychelles, respectively. Previous records of *T. aurantium* from California have been reclassified into two new species: *T. californiana* de Laubenfels, 1932 and *T. vacua* Austin et al., 2014. Similarly, former *T. aurantium* specimens from Brazil have been identified as *T. beatrizae* Ribeiro & Muricy, 2011. In consequence, the occurrence of *T. aurantium* in the Caribbean remains uncertain.

The taxonomic work led by Sarà and collaborators on *Tethya* has resulted in the description of 34 species, which comprise over a third of the current valid species (de Voogd et al., 2024). According to Sarà (1994, 2002), the diagnostic characters that distinguish *Tethya* from the other 13 genera in the family Tethyidae include their spherical or hemispherical body, with a well-developed cortex differentiated from the choanosome, and their main skeleton formed by strongyloxea bundles radiating from the centre of the sponge. The spicule complement of the genus is greatly conserved, containing megascleres (mostly strongyloxeas) and euasters (both megasters and microasters) (Ribeiro & Muricy, 2004; Sarà, 2002; Sarà & Sarà, 2002). Because the terminology for the megasters and microasters has evolved over the years, Ribeiro and Muricy (2011) redescribed the different morphologies and unified the euaster terminology to make comparisons across species from Brazil more detailed and less confusing. This terminology was adopted in later work for a new species from Brazil (Mácola & Menegola, 2018), but it has not been used in subsequent descriptions of new *Tethya* species from other regions (Austin et al., 2014; Hajdu et al., 2013; Sorokin et al., 2019), where the authors still used the classic terms (Boury-Esnault & Rützler, 1997; Sarà, 1994, 2002).

Pioneering work on the evolutionary framework of *Tethya* was also developed by Sarà (1987), who compiled the main character variation within the genus including morphological, ecological, cytological, biochemical, reproductive, and biogeographic traits. This study exposed some of the main gaps of information and envisaged the presence of cryptic species within the widely distributed species *T. aurantium*, *T. seychellensis*, and *T. japonica* Sollas, 1888 (Sarà, 1987). Bergquist and Kelly-Borges (1991) built the first phylogeny of *Tethya* based on morphological characters, mainly with Australian and New Zealand species. Their work highlighted the need to use standard terminology and revealed that well-defined characters such as the arrangement of megascleres, spheraster shape, colour, and the regularity or deformity of microasters, among others, had high consistency index values, hence being highly informative in phylogenetic analyses. The exercise was repeated by Sarà and Sarà (2004) with a larger

number of species also from the Austral region and showed a correspondent arrangement of species groups within *Tethya*. A similar cladistic approach was used for the reconstruction of a family-level phylogeny, suggesting that the speciose genus *Tethya* diverged early in the evolution of the Tethyidae with successive branching of monospecific or less speciose genera in the family (Sarà & Burlando, 1994).

Subsequent attempts to reconstruct the phylogeny of *Tethya* included the combination of a single molecular marker (*cytochrome* c *oxidase subunit I*, COI) and morphological characters (Heim et al., 2007), and with few exceptions, the groups recovered by the molecular analyses correspond to those found using morphological characters. Since then, some of the new *Tethya* species have been described including molecular data and, therefore, subsequent reexaminations of the phylogeny have been conducted (Heim & Nickel, 2010; Sorokin et al., 2019). In the most recent study, Sorokin et al. (2019) discussed the possibility of using external colour as a diagnostic character for some clades, and, given the lack of other synapomorphies, they proposed that the exploration of chemical compounds, specialized cells, and associated microbes could provide additional insights on the phylogenetic relationships of the different lineages in the family.

The sponge microbiome is well-known for being species-specific (Thomas et al., 2016, Yang et al., 2019) and even genotype-specific (Griffiths et al., 2019; Díez-Vives et al., 2020; Easson et al., 2020), and also showing strong functional convergence of the microbiome roles (Fan et al., 2012). Two ecological sponge types were described based on their microbial abundance, diversity, and pumping rate (Vacelet & Donadey, 1977). One type, termed 'Low Microbial Abundance' (LMA) sponges, has a microbial concentration close to that of seawater, and these sponges rely on heterotrophic feeding on particulate organic matter. The second type, 'High Microbial Abundance' (HMA) sponges, can contain microbial communities occupying up to 80% of their tissues in some species, and these sponges rely on this microbiome to acquire nutrients (Hentschel et al., 2006; Weisz et al., 2007; Pankey et al., 2022). While the LMA sponges harbour microbiota of very diverse phylogenetic signatures (Sipkema et al., 2015, Thomas et al., 2016), the HMA sponges are dominated by a few microbial phyla (Moitinho-Silva, Nielsen et al., 2017; Pita et al., 2018). *Tethya* species are consistently considered to be LMA, either by using predictive methodologies (Moitinho-Silva, Steinert et al., 2017; Pankey et al., 2022), by 16S rRNA amplicon sequencing (Thiel et al., 2007; Waterworth et al., 2017), or by direct ultrastructural observation of tissues (Gaino et al., 2006; Gaino & Sarà, 1994). Microbiomes can be vertically transmitted to the offspring through oocytes, which secure necessary symbionts during the settlement phase, or horizontally acquired from the environment by filtration, or a combination of both (Schmitt et al., 2008; Vrijenhoek, 2010; Ebert, 2013; de Oliveira et al., 2020). Given that several studies have reported vertical transmission of symbionts in Mediterranean species of *Tethya* (Gaino et al., 1987; Gaino & Sarà, 1994; Sciscioli et al., 2002), and following up on the idea by Sorokin et al. (2019), we explored how the microbiome signatures can potentially serve as an additional feature to aid in the systematics of sponges, in the genus *Tethya* in particular.

Here, we describe the morphological features of four new species of the genus *Tethya* from the Caribbean, North and South Atlantic, and the Persian Gulf, and place them in a molecular phylogenetic framework. In addition, we analyse the microbiome of the new species and additional sympatric *Tethya* species to understand phylosymbiotic patterns in this cosmopolitan sponge genus.

Materials and methods

Several specimens of two morphospecies (preliminarily identified as *Tethya*) were collected on coral reefs in Isla Cristóbal, Bocas del Toro, Panama (9.21685, −82.21370) in March 2010 by scuba diving (Table 1) and three more in the intertidal area of Pituba Beach, Salvador de Bahia, Brazil (–13.0066632, −38.4547663) in January 2018. Three specimens of an undescribed *Tethya* species were also collected in a rocky shore in the 'corrales' of Chipiona, Cádiz, Spain (36.74168, −6.43887) and subtidal pools in La Palma, Canary Islands (28.693245, −17.759086) by snorkelling, in October 2014 and September 2022, respectively. A specimen collected in 1998 in the Persian Gulf, Ras Ghumeis, United Arab Emirates (24.380880, 51.576362) and deposited at The Natural History Museum, London, UK (NHMUK) under voucher number 2000.9.14.16 was also examined (Table 1). All newly collected specimens were fixed in 96% ethanol soon after collection. To compare the morphological and molecular features of the new species, several other *Tethya* specimens, including type material from the collections of the NHMUK, were examined (Table 1).

Spicules were prepared by dissociation in sodium hypochlorite, followed by two washes with water, and one with 96% ethanol. Microscope slides of the spicules were prepared and permanently mounted with DPX (distyrene, plasticizer, and xylene) medium. Thick sections for most species were prepared using tissue embedded in paraffin, sectioned with a microtome at 10 µm,

Table 1. Metadata for all specimens considered in the phylogenetic analyses, including species name (and label in the tree), collection localities, voucher and accession numbers for both COI and 28S, and whether microbiome sequencing was included.

Species	Name in trees	Locality	Voucher/Sample name	COI Accession number	28S Accession number	16S amplicon Accession number
Adreus fascicularis	*Adreus fascicularis* HQ379428 or HQ379314	English Channel, UK	Mc4559	HQ379428	HQ379314	NO
Adreus micraster	*Adreus micraster* AY626306	Mauritania	POR06837		AY626306	NO
Adreus sp.	*Adreus* sp. HQ379377	Ireland	BELUM:Mc4982		HQ379377	NO
Axos cliftoni	*Axos cliftoni* KY947263	Vietnam: Quang Tri	MT5.2015	KY947263		NO
Axos cliftoni	*Axos cliftoni* AY626308	Australia	G300111		AY626308	NO
Axos cliftoni	*Axos cliftoni HQ379380*	Australia	BELUM:POR06166		HQ379380	NO
Axos flabelliformis	*Axos flabelliformis* KC869578	Australia	NCI089		KC869578	NO
Cliona celata	*Cliona celata* KY492595	Portugal	M23F	KY492595		NO
Jaspis sp.	*Jaspis* sp. *AY561977*	Papua New Guinea	UCMPWC1021	AY561977		NO
Adreus sp.	*Adreus* sp. AY561901	Australia	G315767		AY561901	NO
Laxotethya dampierensis	*Laxotethya dampierensis* AY561905	Australia	WAMZ11871		AY561905	NO
Liosina blastifera	*Liosina blastifera* KX866762	Israel: Ma'agan-Mikha'el	Po.25551	KX866762		NO
Liosina paradoxa	*Liosina paradoxa* AF437303 or *AY319318*	Sulawesi/Indonesia		AF437303	AY319318	NO
Paratimea hoffmanae	*Paratimea hoffmanae* KC869429	Norway: Røst reef	ZMBN 125735	KC869429		NO
Placospongia intermedia	*Placospongia intermedia* JX999089	Panama: Bocas del Toro	MCZ:DNA106621	JX999089		NO
Placospongia sp.	*Placospongia* sp. KC869430	Panama: Bocas del Toro	PC-BT-18	KC869430		NO
Stellitethya ingens	*Stellitethya ingens* AY561899	Australia	WAMZ11947		AY561899	NO
Tectitethya keyensis	*Tectitethya keyensis* KC869616	USA	NCI360		KC869616	NO
Tethya actinia	*Tethya actinia* AY320033	USA: Zane Grey Creek, Long Key, Florida		AY320033		NO
Tethya actinia	*Tethya actinia* i1	Panama: Bocas del Toro	*MCZ:IZ:135213_2*	PP594403		PRJNA970968
Tethya actinia	*Tethya actinia* i2	Panama: Bocas del Toro	*MCZ:IZ:135213_3*	PP594404		PRJNA970968
Tethya actinia	*Tethya actinia* i3	Panama: Bocas del Toro	*MCZ:IZ:135213_1*	NO		PRJNA970968
Tethya aurantium	*Tethya aurantium* JX999070	Italy: Bari	MCZ:ICZ:DNA106628	JX999070		NO
Tethya aurantium	*Tethya aurantium* EF558571	Croatia		EF558571		NO
Tethya aurantium	*Tethya aurantium* EF093531	Croatia		EF093531		NO

(*Continued*)

Table 1. Continued.

Species	Name in trees	Locality	Voucher/Sample name	COI Accession number	28S Accession number	16S amplicon Accession number
Tethya aurantium	*Tethya aurantium* EF093529	Croatia		EF093529		NO
Tethya aurantium	*Tethya aurantium* EF584565	Elba, Italy		EF584565		NO
Tethya aurantium	*Tethya aurantium* i6	Italy: Naples	MCZ:ICZ:106628	OQ948196	OQ947274	PRJNA970968
Tethya aurantium	*Tethya aurantium* i7	Italy: Naples		OQ948197	OQ947273	PRJNA970968
Tethya aurantium	*Tethya aurantium* i8	Italy: Naples				PRJNA970968
Tethya aurantium	*Tethya aurantium i9*	Italy: Naples		OQ948198		PRJNA970968
Tethya aurantium	*Tethya aurantium* i10	Italy: Naples				PRJNA970968
Tethya bergquistae	*Tethya bergquistae*	New Zealand: Wellington		OQ948203		NO
Tethya burtoni	*Tethya burtoni*	New Zealand: Wellington		OQ948210		NO
Tethya californiana	*Tethya californiana* AY561978 or AY561900	USA: Carmel, California		AY561978	AY561900	NO
Tethya californiana	*Tethya californiana* KJ620403	South Australia		KJ620403		NO
Tethya californiana	*Tethya californiana* GQ292532	Canada: Vancouver Island	BCA1	GQ292532		NO
Tethya californiana	*Tethya californiana* GQ292533	Canada: Vancouver Island	BCA2	GQ292533		NO
Tethya cf. *aurantium*	*Tethya* cf. *aurantium* AY552024	France: Marseille			AY552024	NO
Tethya citrina	*Tethya citrina* EF558570	UK: Northern Ireland	MC3217	EF558570		NO
Tethya citrina	*Tethya citrina* HQ379427 or HQ379237	UK: Wales	Mc5113	HQ379427	HQ379237	NO
Tethya citrina	*Tethya citrina* EF558569	Croatia	SPD279	EF558569		NO
Tethya citrina	*Tethya citrina* i4	Italy: Naples	US113	OQ948205	OQ947272	NO
Tethya citrina	*Tethya citrina* i5	France: Roscoff	Roscoff 2		OQ947284	PRJNA970968
Tethya citrina	*Tethya citrina* i6	France: Roscoff	Roscoff 10		OQ947285	PRJNA970968
Tethya citrina	*Tethya citrina* i7	Spain: Ría de Vigo, Galicia	Gali1	OQ948206		PRJNA970968
Tethya citrina	*Tethya citrina* i8	Spain: Ría de Vigo, Galicia	Gali2			PRJNA970968
Tethya citrina	*Tethya citrina* i9	Spain: La Palma, Canary Islands	MNCN 1.01/1041	PP587641		PRJNA970968
Tethya citrina	*Tethya citrina* i10	Spain: La Palma, Canary Islands	MNCN 1.01/1042	PP587642		NO
Tethya citrina	*Tethya citrina* i11	Spain: La Palma, Canary Islands	MNCN 1.01/1043	PP587638		PRJNA970968

(*Continued*)

Table 1. Continued.

Species	Name in trees	Locality	Voucher/Sample name	COI Accession number	28S Accession number	16S amplicon Accession number
Tethya citrina	*Tethya citrina* i12	Spain: La Palma, Canary Islands	MNCN 1.01/1044	PP587640		PRJNA970968
Tethya citrina	*Tethya citrina* i13	Spain: La Palma, Canary Islands	MNCN 1.01/1045	PP587639		PRJNA970968
Tethya coccinea	*Tethya coccinea* JQ034584	Australia: Queensland	G303083	JQ034584		NO
Tethya erici sp. nov.	*Tethya erici* sp. nov. i1	Spain: Chipiona	MNCN 1.01/1023	OQ948204	OQ947278	PRJNA970968
Tethya erici sp. nov.	*Tethya erici* sp. nov. i2	Spain: Chipiona	MNCN 1.01/1024			PRJNA970968
Tethya erici sp. nov.	*Tethya erici* sp. nov. i3	Spain: Chipiona	MNCN 1.01/1025			PRJNA970968
Tethya erici sp. nov.	*Tethya erici* sp. nov. i4	Spain: La Palma, Canary Islands	MNCN 1.01/1027	PP587635		PRJNA970968
Tethya erici sp. nov.	*Tethya erici* sp. nov. i5	Spain: La Palma, Canary Islands	MNCN 1.01/1028	PP587627		PRJNA970968
Tethya erici sp. nov.	*Tethya erici* sp. nov. i6	Spain: La Palma, Canary Islands	MNCN 1.01/1029	PP587633		PRJNA970968
Tethya erici sp. nov.	*Tethya erici* sp. nov. i7	Spain: La Palma, Canary Islands	MNCN 1.01/1030	PP587634		NO
Tethya erici sp. nov.	*Tethya erici* sp. nov. i8	Spain: La Palma, Canary Islands	MNCN 1.01/1031	PP587636		NO
Tethya erici sp. nov.	*Tethya erici* sp. nov. i9	Spain: La Palma, Canary Islands	MNCN 1.01/1032	PP587624		NO
Tethya erici sp. nov.	*Tethya erici* sp. nov. i10	Spain: La Palma, Canary Islands	MNCN 1.01/1033	PP587626		NO
Tethya erici sp. nov.	*Tethya erici* sp. nov. i11	Spain: La Palma, Canary Islands	MNCN 1.01/1034	PP587628		NO
Tethya erici sp. nov.	*Tethya erici* sp. nov. i12	Spain: La Palma, Canary Islands	MNCN 1.01/1035	PP587625		NO
Tethya erici sp. nov.	*Tethya erici* sp. nov. i13	Spain: La Palma, Canary Islands	MNCN 1.01/1036	PP587629		NO
Tethya erici sp. nov.	*Tethya erici* sp. nov. i14	Spain: La Palma, Canary Islands	MNCN 1.01/1037	PP587630		NO
Tethya erici sp. nov.	*Tethya erici* sp. nov. i15	Spain: La Palma, Canary Islands	MNCN 1.01/1038	PP587631		NO
Tethya erici sp. nov.	*Tethya erici* sp. nov. i16	Spain: La Palma, Canary Islands	MNCN 1.01/1039	PP587632		NO
Tethya erici sp. nov.	*Tethya erici* sp. nov. i17	Spain: La Palma, Canary Islands	MNCN 1.01/1040	PP587637		NO
Tethya gracilis	*Tethya gracilis* EF584568	Germany: Aquazoo Loebekke-Museum, Düsseldorf		EF584568		NO
Tethya gracilis	*Tethya gracilis* i1	Brazil: Salvador de Bahia	UFBAPOR 5021	OQ948213		PRJNA970968
Tethya gracilis Chengue	*Tethya gracilis* i2	Colombia: Chengue Bay, Colombia	INV-PSM492	OQ948212	OQ947276	PRJNA970968
Tethya hibernica	*Tethya hibernica* EF558566	UK: Northern Ireland: Rathlin Island	Mc2426	EF558566		NO

(*Continued*)

Table 1. Continued.

Species	Name in trees	Locality	Voucher/Sample name	COI Accession number	28S Accession number	16S amplicon Accession number
Tethya hibernica	*Tethya hibernica* EF558567	UK: Northern Ireland: Rathlin Island	Mc3037	EF558567		NO
Tethya hibernica	*Tethya hibernica* EF558568	UK: Northern Ireland: Rathlin Island	Mc2486	EF558568		NO
Tethya hibernica	*Tethya hibernica HQ379238*	UK: Northern Ireland: Rathlin Island	Mc4061		HQ379238	NO
Tethya irisae	*Tethya irisae* MH518072 or MH511148	South Australia: Great Australian Bight	SAMA S2913	MH518072	MH511148	NO
Tethya martini sp. nov.	*Tethya martini* sp. nov. i1	Panama: Bocas del Toro	MCZ:IZ:133702	OQ948211	OQ947275	PRJNA970968
Tethya martini sp. nov.	*Tethya martini* sp. nov. i2	Panama: Bocas del Toro	MCZ:IZ:135212_2	PP594405		PRJNA970968
Tethya martini sp. nov.	*Tethya martini* sp. nov. i3	Panama: Bocas del Toro	MCZ:IZ:135212_1	PP594406		NO
Tethya minuta	*Tethya minuta* EF584567	Germany: Vivarium of the Museum for Natural History, Karlsruhe		EF584567		NO
Tethya norvegica	*Tethya norvegica* EF558565	Norway: Trondheimfjord		EF558565		NO
Tethya norvegica	*Tethya norvegica* i2	UK: Rockall Bank, UK EEZ	Rockall Bank 1 (22) i2 = SP14348001	OQ948207	OQ947281	PRJNA970968
Tethya norvegica	*Tethya norvegica* i3	UK: Rockall Bank, UK EEZ	UPSZMC 190662	OQ948208	OQ947282	PRJNA970968
Tethya norvegica	*Tethya norvegica* i4	UK: Rockall Bank, UK EEZ	UPSZMC 190664	OQ948209	OQ947283	NO
Tethya orioni sp. nov.	*Tethya orioni* sp. nov. i1	United Arab Emirates: Ras Ghumeis	NHMUK 2000.9.14.16	OQ948214	OQ947277	PRJNA970968
Tethya samaaii	*Tethya samaaii* KX618511	South Africa	TIC2016_003		KX618511	NO
Tethya seychellensis	*Tethya seychellensis* EF584569	Vietnam: Halong Bay, Hang Du Lake		EF584569		NO
Tethya seychellensis	*Tethya seychellensis* KC869475	Panama: Bocas del Toro	P09		KC869475	NO
Tethya simoni sp. nov.	*Tethya* sp. KC869527	Solarte Mangroves, Bocas del Toro, Panama			KC869527	NO
Tethya simoni sp. nov.	*Tethya simoni* sp. nov. i1	Panama: Bocas del Toro	MCZ:IZ:133701	OQ948199	OQ947279	PRJNA970968
Tethya simoni sp. nov.	*Tethya simoni* sp. nov. i2	Brazil: Salvador de Bahia	UFBAPOR 5019	OQ948200		NO
Tethya simoni sp. nov.	*Tethya simoni* sp. nov. i3	Brazil: Salvador de Bahia	UFBAPOR 5020	OQ948202	OQ947280	NO
Tethya simoni sp. nov.	*Tethya simoni* sp. nov. i4	Brazil: Salvador de Bahia	UFBAPOR 5022	OQ948201		PRJNA970968
Tethya simoni sp. nov.	*Tethya simoni* sp. nov. i5	Panama: Bocas del Toro	MCZ:IZ:135212_3	PP594407		PRJNA970968

(*Continued*)

Table 1. Continued.

Species	Name in trees	Locality	Voucher/Sample name	COI Accession number	28S Accession number	16S amplicon Accession number
Tethya simoni sp. nov.	*Tethya simoni* sp. nov. i6	Panama: Bocas del Toro	MCZ:IZ:135212_4	PP594408		PRJNA970968
Tethya sp. 1 MW016333	Tethya sp. 1 MW016333	USA: Hawaii	UF4067		MW016333.1	NO
Tethya sp. 2 MW016337	Tethya sp. 2 MW016337	USA: Hawaii	KBOA04101728		MW016337	NO
Tethya sp. 3 MW016339	Tethya sp. 3 MW016339	USA: Hawaii	UF3981		MW016339.1	NO
Tethya sp. 5 MW016342	Tethya sp. 5 MW016342	USA: Hawaii	KBOA0921711		MW016342.1	NO
Tethya sp. 6 MW016346	Tethya sp. 6 MW016346	USA: Hawaii	UF3842		MW016346.1	NO
Tethya sp. 7 MW016348	Tethya sp. 7 MW016348	USA: Hawaii	UF3919		MW016348.1	NO
Tethya sp. 8 KX866754	*Tethya* sp. 8 KX866754	Israel: Ma'agan-Mikha'el	Po.25553	KX866754		NO
Tethya sp. 9 KJ620390	*Tethya* sp. 9 KJ620390	Australia	190513-05		KJ620390	NO
Tethya sp. 10 KU060331	*Tethya* sp. 10 KU060331	Saudi Arabia: Red Sea, JazAir Sila	SNSB-BSPG.GW26962		KU060331	NO
Tethya sp. 11 KU060339	*Tethya* sp. 11 KU060339	Saudi Arabia: Red Sea, Gulf of Alqaba	BSPG-SNSB.GW26972		KU060339	NO
Tethya sp. 12 KU060339/KU060752	*Tethya* sp. 12 KU060339/KU060752	Saudi Arabia: Red Sea, Gulf of Aqaba	BELUM:Mc5113		KU060339	NO
Tethya sp. 13 KU060536	*Tethya* sp. 13 KU060536	Saudi Arabia: Red Sea, Qunfudhah	BSPG-SNSB.GW6033	KU060752	KU060536	NO
Tethya sp. 14 KU060640	*Tethya* sp. 14 KU060640	Saudi Arabia: Red Sea, Al Wajh	BSPG-SNSB.GW3401	KU060640		NO
Tethya sp. 15_ MZ487256	Tethya sp. 15_ MZ487256	Caribbean PANKEY	NZCC2	MZ487256		NO
Tethya stellagrandis	*Tethya stellagrandis* AY561920	Maldives	POR15727		AY561920	NO
Tethya wilhelma	*Tethya wilhelma* EF584570	Germany: Zoological-Botanical Garden 'Wilhelma', Stuttgart		EF584570	c34318_g4_i4 (from transcriptome)	NO
Tethyidae sp. AY561904	Tethyidae sp. AY561904		UCMPWC957		AY561904	NO
Tethyidae sp. AY561986	Tethyidae sp. AY561986		UCMPWC1062	AY561986		NO
Tethyidae sp. AY626310	Tethyidae sp. AY626310	Australia	G304645		AY626310	NO
Tethytimea carmelita	*Tethytimea carmelita* KY130425	Mexico: Campeche	LEB-ICML-UNAM-3133		KY130425	NO
Timea cf. *centrifera*	*Timea* cf. *centrifera* AY561906	Australia	WAMZ9801		AY561906	NO
Timea sp. AY561907	*Timea* sp. AY561907		G303973		AY561907	NO

(*Continued*)

Table 1. Continued.

Species	Name in trees	Locality	Voucher/Sample name	COI Accession number	28S Accession number	16S amplicon Accession number
Timea sp. AY626300	*Timea* sp. AY626300		UCMPWC957		AY626300	NO
Timea sp. AY626303	*Timea* sp. AY626303		G313459		AY626303	NO
Timea unistellata	*Timea unistellata* KC869427	Ireland	BELUM:Mc7300	KC869427		NO
Trachycladus laevispirulifer	*Trachycladus laevispirulifer* AY626305	Australia	WAMZ1186		AY626305	NO
Trachycladus stylifer	*Trachycladus stylifer* KC869453	New Zealand	NCI301		KC869453	NO
Xenospongia patelliformis	*Xenospongia patelliformis* KC869650	Maldives	NCI335		KC869650	NO

stained with haematoxylin and mounted in DPX. Images were taken on an Olympus BX43 light microscope with a UC50 camera. Additional spicules were mounted on SEM stubs, coated with gold, and imaged under a Zeiss UltraPlus scanning electron microscope (SEM) at the NHMUK. Measurements for megascleres were taken from light microscopy images, while measurements for megasters/microsters were taken from SEM images using the software ImageJ (Schneider et al., 2012). All measurements were obtained from the holotype specimens unless otherwise indicated.

DNA extraction, amplification, and sequencing

Following the protocols of the Sponge Barcoding Project (www.spongebarcoding.org), we sequenced two molecular makers, the standard mitochondrial COI fragment (Folmer et al., 1994) and a fragment of the 28S rRNA ribosomal gene (28S rRNA), using the primer pair Por28S15F—Por28S1520R (Morrow et al., 2012). This encompassed 51 specimens from 11 putative species (Table 1). Small fragments of choanosomal tissue were used for DNA extraction using the Qiagen™ Blood and Tissue extraction kit, following the manufacturer's instructions. Spicules were removed by adding one spinning step after lysis and before transferring the mixture into the Qiagen columns. The quality and quantity of resulting extracts were checked with a NanoDrop spectrophotometer.

The PCR programme for COI was 94 °C for 5 min, 5 cycles (94 °C for 30 s, 45 °C for 1.5 min, 72 °C for 1 min), 35 cycles (94 °C for 30 s, 50 °C for 1.5 min, 72 °C for 1 min) and final extension at 72 °C for 7 min (Cárdenas et al., 2010). The PCR programme for 28S rRNA was 94 °C for 5 min, 30 cycles (94 °C for 30 s, 53 °C for 30 s, 72 °C for 30 s) and final extension at 72 °C for 5 min (Morrow et al., 2012). Amplification of both COI and 28S rRNA markers was performed in 12.5 µl reactions, using 10.5 µl of VWR Red Taq DNA Polymerase 1.1× Master Mix (VWR International bvba/sprl, Belgium), 0.5 µl of the forward and reverse primers, and 1 µl of DNA template. PCR products were verified by gel electrophoresis on 1.5% agarose. Purification and sequencing of PCR products were conducted at the Molecular Core Labs (Sequencing Facility) of the NHMUK.

Individual reads were assembled and trimmed into consensus sequences using the software Geneious v.2021.1.10 (https://www.geneious.com). In a few cases, only forward or reverse sequences were used due to the poor quality of one of the sequencing reactions. Consensus sequences were checked for contamination

using BLAST (Madden, 2002). Available sequences of *Tethya* and Tethyidae were downloaded from GenBank. Alignment was performed with the multiple sequence alignment program, MAFFT v.7.309 (Katoh & Standley, 2013). The alignment for COI contained 658 bp for 84 taxa while the alignment for 28S rRNA contained 1500 characters for 54 taxa. Phylogenetic analyses were conducted using maximum likelihood in RAxML 8.1.22 (Stamatakis, 2014). The best-fit model of evolution was selected using jModelTest (Darriba et al., 2012), resulting in HKY + I+G4 model for COI and GTR + I model for 28S rRNA. Phylogenetic analyses for COI and 28S rRNA were run separately 10 times, with 100 bootstrap replicates. Additional COI sequences of *T. burtoni* Sarà & Sarà, 2004 and *T. bergquistae* Hooper in Hooper & Wiedenmayer, 1994 from Australian waters were also included in the analyses (Table 1), although not directly sequenced in this study. Raw sequences for COI and 28S generated in this study were deposited at GenBank (Table 1).

Microbiome composition and structure

16S rRNA amplification. For 33 specimens of 9 species of *Tethya*, we targeted the V4 hypervariable region of the 16S rRNA gene to study the composition and structure of their microbiome. The V4 region was amplified using general bacterial primers 515 F-Y (Parada et al., 2016) and 806 R (Apprill et al., 2015), with the Illumina adapter overhang sequences in both primers and dual-barcoding approach (Kozich et al., 2013). These primers contain degenerate bases to avoid the previous bias against Crenarchaeota/Thaumarchaeota and the Alphaproteobacterial clade SAR11. We used the PCRBIO HiFi Polymerase (PCR Biosystems Ltd) under the following conditions: 95 °C for 3 min, followed by 28 cycles of 95 °C for 20 s, 60 °C for 20 s and 72 °C for 30 s, after which a final elongation step at 72 °C for 5 min was performed. DNA amplification was done in duplicates, and PCR products were checked on a 1% agarose gel to determine the success of amplification and the relative intensity of bands. PCR products were purified with Agencourt AMPure XP Beads (Beckman Coulter Inc.), and libraries prepared with the Nextera XT DNA Library Preparation Kit (Illumina Inc.). An equimolar pool of DNA was generated by normalizing all samples at 4 nM for sequencing. Next-generation, paired-end sequencing was performed at the NHMUK on an Illumina MiSeq using v3 chemistry (2 × 300 bp). Raw amplicon sequence reads were deposited at the Sequence Read Archive (SRA) with BioProject accession ID PRJNA970968.

Read processing, taxonomic assignment, and core ASVs. Raw paired reads were imported into Mothur (v.1.41.3), and an adaptation of the MiSeq SOP protocol was followed (Kozich et al., 2013). Briefly, primer sequences were removed and sequence contigs were built from overlapping paired reads. The merged amplicon sequence lengths were ca. 298 bp for the V4 region. Sequences with >0 N bases or with >15 homopolymers were discarded. Unique sequences were aligned against the Silva reference data set (release 132), and poorly aligned sequences were removed. Unoise3 (Callahan et al., 2017), implemented within Mothur, was used for denoising (i.e., error correction) of unique aligned sequences, to infer amplicon sequence variants (ASVs), allowing one mismatch per 100 bp (Oksanen et al., 2018). Any singletons remaining at this stage were removed. Reference-based chimaera checking was conducted using UCHIME with the Silva reference data set and parameter minh = 0.3. ASVs were classified using the Silva database v.132, with a cut-off value of 80. ASVs classified as eukaryotic-chloroplast-mitochondria or unknown were discarded, these represented 0.08% of sequences. Community sampling efficiency was examined using rarefaction curves.

Statistical design and analysis. Description of the microbial community was done using the total number of ASVs transformed to relative abundances (RA) for each individual. The core microbiome was determined on the rarefied data as the ASVs that were present in 70% of samples at any abundance, and among the phylogenetic clusters defined using the COI gene. Measures of ASV richness and Shannon index were calculated using rarefied samples in R v.4.0.5. Analysis of variance (ANOVA) was performed to compare alpha diversity among both *Tethya* clades and species, and Tukey's honestly significant difference (HSD) was used for addressing pairwise comparisons. Beta diversity was calculated using the Bray–Curtis dissimilarity coefficient on RA transformed ASVs with a minimum of 0.01% RA across samples (these included 89–98% of the total RA). The relative abundances were log2 transformed prior to the calculation of Bray–Curtis dissimilarities. These dissimilarity matrices were visualized using Principal coordinates analysis (PcoA) using '*cmdscale*' in vegan v. 2.5–7 (De Cáceres & Legendre, 2009). Permutational Analysis of Variance (PERMANOVA), using the *adonis* function of the 'vegan' package, was used to examine differences in microbial composition between *Tethya* clades. Microbial orders that were differentially abundant between the taxonomic clades and between the *Tethya* species were identified in pairwise comparisons using the '*TukeyHSD*' package in R.

Orders with an adjusted (i.e., Benjamini–Hochberg corrected) *p*-value of less than 0.05 were considered differential between groups.

Museum acronyms. SNSB-BSPG, Bayerische Staatssammlung für Paläontologie und Geologie, Munich, Germany; INV, Museo de Historia Natural Marina de Colombia, Invemar, Santa Marta, Colombia; LEB-ICML-UNAM, Colección de Esponjas of the Instituto de Ciencias del Mar y Limnología, Universidad Nacional Autónoma de México, México DF, México; MCZ, Museum of Comparative Zoology, Harvard University, Cambridge, MA, USA; MNRJ, Museu Nacional da Universidade Federal do Rio de Janeiro, Rio de Janeiro, Brazil; NHMUK, The Natural History Museum, London, UK; MNHN, Muséum national d'Histoire naturelle, Paris, France; MSNG, Museo Civico di Storia Naturale di Genova 'Giacomo Doria', Genova, Italy; SAM, South Australian Museum, Adelaide, South Australia, Australia; UCPM, University of California Museum of Paleontology, Berkeley, CA, USA; UPSZMC, Zoology collections of the Museum of Evolution, Uppsala University, Uppsala, Sweden; WAM, Western Australian Museum, Perth, Western Australia, Australia; UFBAPOR, Museu de História Natural da Bahia, Salvador, Bahia, Brazil.

Results

Systematics

Class DEMOSPONGIAE Sollas, 1885
Order TETHYIDA Morrow & Cárdenas, 2015
Family TETHYIDAE Gray, 1848
Genus *Tethya* Lamarck, 1814

Tethya martini Riesgo, Giribet & Santodomingo, sp. nov.
ZooBank registration: urn:lsid:zoobank.org:act:412FE7B6-BDE5-4678-8665-B4C11326168A
Fig. 1

Examined material: Holotype MCZ:IZ:133702 (DNA in Biobank with number DNA106632), Bahía de los Delfines (9.21685, −82.21370), Isla Cristóbal, Bocas del Toro, Panama, 5 m deep, leg. A. Riesgo & G. Giribet, 15 Mar 2010. Paratypes MCZ:IZ:135212 1 and 2 (DNA in Biobank with number DNA106830), two specimens, same locality as holotype, leg. G. Giribet, 13 Mar 2012.

Diagnosis. *Tethya* with bright red colour, thin cortex, and no spheraster. Two types of microsters present: strongylasters and tylasters; spherasters absent.

Description. Body of holotype and paratypes hemispherical to spherical, 6–8 mm in diameter by 5–6 mm high (Fig. 1A and Table 2), attached to substrate by short lateral extensions of the base. External colour *in vivo* bright red (Fig. 1A and Table 2), whitish in ethanol. Cortical surface covered by flattened, polygonal tubercles with regular size, 0.4–0.5 mm in diameter by 0.3–0.4 mm high, homogeneously distributed and separated by reticulate areas. Some buds protrude from tubercles, 100–150 µm in diameter, stalked by thin peduncles 1.1–2.1 mm long (Fig. 1A and Table 2). Oscules 0.5–1 mm in diameter, generally located in the apex or laterally in the sponge body, if more than one; holotype with a single apical oscule and paratype with up to three, one apical and two lateral.

Skeleton. Cortex about 0.4 mm thick (holotype and paratypes) with lacunae. Radial bundles of megascleres, approximately 200 µm thick, ending in fan-shaped expansions of the cortex, subdivided into 2–3 fascicles. Without megasters in the cortex or choanoderm. Tylasters present in both the choanosome and the cortex, and strongylasters more prevalent in the choanoderm (Table 2).

Spicules. Holotype. Megascleres, main strongyloxeas with rounded or hastate ends, straight or slightly bent, 700.5-884.8-1174.5 µm long by 8.2-13.6-18.8 µm wide (Fig. 1A–B, Supplemental Fig. S1A); accessory strongyloxeas with rounded or hastate ends, 407.2-473-592.4 µm long by 5.6-7.3-10 µm wide; no spherasters. Microscleres, strongylasters, and tylasters of similar size (Fig. 1E–G). Strongylasters type 1 and type 2 with similar sizes, 9.5-11.1-12.7 µm in diameter, with small nucleus 2.5-2.9-3.3 µm, and 10-12-15 straight, cylindrical rays spined in their distal ½ portion, with rounded and sometimes bifurcated ends (strongylaster type 1, Fig. 1E) or 10-12-15 slightly conical rays (4.3-4.7-5.5 µm in length by 0.7-0.9-1.1 µm in width) with larger, sharper spines, along their ⅔ distal portion (strongylaster type 2, Fig. 1F). Tylasters (Fig. 1G) 8.4-9.7-10.9 µm in diameter, with slightly larger nucleus 2.7-3.2-3.7 µm, and 10-12-15 straight, short, cylindrical rays enlarged at the tips; rays 3.0-3.7-4.3 µm long by 0.9-1.1-1.2 µm wide, bearing high spines with rounded tips along the ¾ or ½ of the rays, although in larger density at ¼ tips (Table 2).

Distribution and ecology. *Tethya martini* sp. nov. has been found in shallow coral reefs in Bocas del Toro (Panama), in crevices among rubble of the scleractinian *Porites porites* (Pallas, 1766), at a depth of <5 m.

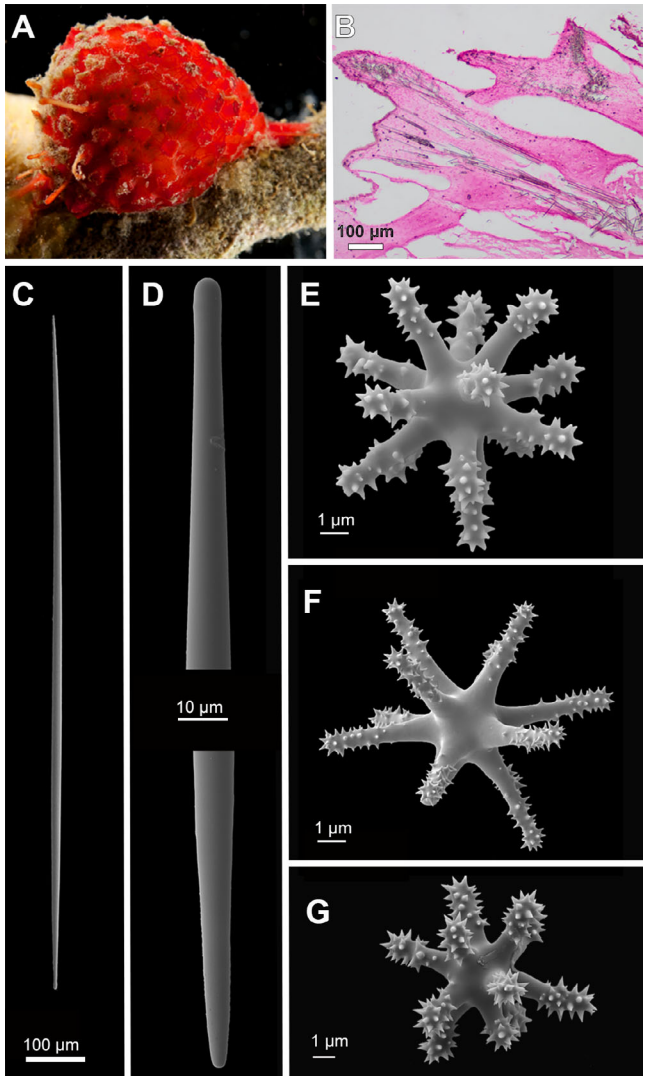

Fig. 1. *Tethya martini* sp. nov. MCZ:IZ:133702. A. Field image of a live specimen. B. Skeletal architecture of cortex and upper choanosome in cross section. C. Strongyloxea, slightly bent. D. Strongyloxea, rounded and hastate tips. E. Strongylaster type 1. F. Strongylaster type 2. G. Tylaster.

Remarks. The lack of spherasters (or megasters) in *T. martini* sp. nov. is a character shared with *T. fastigata* Bergquist & Kelly-Borges, 1991 and *T. amplexa* Bergquist & Kelly-Borges, 1991 from New Zealand (Bergquist & Kelly-Borges, 1991), as well as with the genus *Oxytethya*. With *T. fastigata*, it shares the brick-red colour when alive and a low density of microscleres in the choanosome, but *T. fastigata* differs in having deformed micrasters (∼polyrhabds) and abundant oxyasters. *Tethya amplexa* has a distinct yellow colour, and a high density of micrasters and oxyasters, all features different from the new species. *Tethya martini* sp. nov. is not a species of *Oxytethya* (which lacks megasters), since the main feature of the genus *Oxytethya*, and present in the only species described so far, *O. mirabilis* Sarà & Sarà, 2002, is the abundance of oxeas as main (4000–5000 µm) and auxiliary (180–210 µm) megascleres, and polyrhabds among the micrasters (Sarà & Sarà, 2002), both spicule types absent in *T. martini* sp. nov. In addition, *Oxytethya* is only known from SE Australia. We compared *T. martini* sp. nov. with all other species known to occur in the Caribbean, including *T. diploderma* Schmidt, 1870 (NHMUK 1870.5.393, holotype, Supplemental Fig. S2) and the NW Atlantic (NHMUK 1938.4.26.14, Supplemental Fig. S3), *T. taboga* (de Laubenfels, 1936) from Panama (USNM 22216), *T. maza* Selenka, 1879 from Brazil (MNRJ 810, neotype), and *T. simoni* sp. nov. (Table 2, Fig. 2), but all of them possess spherasters (Table 2, Supplemental Figs. S2 and S3), making the absence of spherasters in *T. martini* sp. nov. its main diagnostic character among other species in the region.

Table 2. Diagnostic features for all material described and compared herein.

Species	External appearance/ attachment	Body diameter	Colour	Skeletal arrangement	Spicules	Type locality	Material	Depth (m)	Reference
Tropical Western Atlantic/Northeastern Atlantic/Mediterranean									
Tethya simoni sp. nov.	Hemispherical to spherical, cortex (1.4 mm), reticulated surface	1.2 cm	Orange (*in vivo*), yellow-beige (in ethanol)	Radial bundles of strongyloxeas, 150–250 um thick, form fan-shaped expansions of the cortex, single or subdivided in 2–3 fascicles	Ms = mstrongyloxeas (1107 um), accessory strongyloxeas (480 um), me = spherasters of two sizes (89 and 42 um) with bifurcated and bent rays, mi = strongylaster with 15 rays (14 um), tylasters with 14 rays (12 um), oxyasters with 16 rays (21 um)	Bocas del Toro, Panama	MCZ:ICZ:DNA106631	5 m	This study
Tethya martini sp. nov.	Hemispherical to spherical, cortex (0.5 mm), reticulated surface, tubercles and buds	8 mm	Red (*in vivo*), white (in ethanol)	Radial bundles of megascleres, approximately 200 um thick, ending in fan-shaped expansions of the cortex, subdivided in 2–3 fascicles. Lacunae	Ms = strongyloxeas (884 um), accessory strongyloxeas (473 um), mi = strongylasters type 1 and type 2 with 12 spined rays (11 um) larger in type 1, tylasters with 12 spined rays (9 um)	Bocas del Toro, Panama	MCZ:IZ:DNA106632	5 m	This study
Tethya erici sp. nov.	Spherical, cortex (0.8–1 mm), flattened tubercles, buds	1 cm	Green-yellow (*in vivo*), white (in ethanol)	Radial bundles of megascleres, approximately 250 um thick, ending in fan-shaped expansions of the cortex, not subdivided. Lacunae	Ms = strongyloxeas (860 um), accessory strongyloxeas (340 um), me = spherasters of two sizes (40 um and 15 um) with 7–13 rays, mi = strongylasters in two types of similar size (9 um) and 9 cylindrical rays, strongylaster type 1 with short spines, and strongylaster type 2 with larger spines, tylasters (8 um) and 7–10 rays with sharp, short spines pointing outwards, small oxyasters (9 um) with thin 6–9 rays	Chipiona, Spain	MNCN 1.01/1023	2 m	This study
Tethya actinia	Subspherical, verrucose, lumps (3 mm diameter), buds (1–5 mm), cortex 1 mm thick	5 cm	Bright orange (external and internal)	Fascicles of megascleres to the surface	Ms = Strongyloxeas (2000 × 20 um), me = spherasters (30 um, cen.15 um), chiasters (15 um, 8 rays), oxyasters (32 um, 4–7 rays)	Harrington Sound, Bermuda	NHMUK 1948.8.6.48	Littoral	de Laubenfels & Hindle, 1950
Tethya diploderma	Globular, papillose, roots (1–2 cm)	–	–	Fascicles of megascleres to the surface	Ms = strongyloxeas, me = spherasters (30 um), mi = strongylasters (8.5 um, 6–9 rays)	Antillen	NHMUK 1870.5.393	–	Schmidt, 1870
Tethya diploderma	Globular, hispid, cortex 0.8 cm, tubercles 0.5 cm		Yellow	Ascending tracts of spicules (200 um)	Ms = tylotes (900–1200 um), me = spherasters (67 um),	Panama	USNM 22203		de Laubenfels, 1936

(*Continued*)

Table 2. Continued.

Species	External appearance/ attachment	Body diameter	Colour	Skeletal arrangement	Spicules	Type locality	Material	Depth (m)	Reference
					tylasters (10 um), oxyspherasters (7 um)				
Tethya diploderma		Material of Schmidt, 1870			Ms = mucronate strongyloxeas, me = spherasters (20–30 um), mi = strongylasters type 2, tylasters type 1 (20 um), oxyasters type 2 (14 um), and oxyasters type 3 (16 um)	Gulf of Mexico	MNRJ 12573	–	Ribeiro & Muricy, 2011
Tethya diploderma	–	–	–	Bundles of megascleres (400 um), fanning out at the surface	Me = strongyloxeas (800 um), me = shperasters (30 um), mi = oxyasters type 2 (30 um), tylasters type 1 (8 um)	Bermuda	NHMUK 1938.4.26.14	–	Supplemental Material
Tethya taboga	Subspherical, attached with ribbon-shaped roots (1 cm), tuberculous protrusions (1 mm)	2 cm	Red	Tracts of fascicular megascleres not protruding,	Ms = strongyloxeas or strongyles (600 um), styles (600 um), me = spherasters (65 um), tylasters type I (60 um), oxyasters type I (60 um)	Taboga Island, Pacific Panama	USNM 22216	Littoral	de Laubenfels, 1936
Tethya globum	Globular, smooth	2 cm	Bright orange	Not described	Not described	Guadaloupe, St. Thomas, Viecques	Type lost	littoral	Duchassaing de Fonbressin and Michelotti, 1864
Tethya rubra	Spherical or flattened, smooth surface or tuberculate, thin reticulation, cortex 0.5 mm, very low abundance of spherasters in cortex	2–2.3 cm	Red or yellow externally (*in vivo*), yellow internally	Spicules in poorly organized bundles, sometimes branching out, lacunar cortex	Ms = strongyloxeas (773–960 um), accessory strongyloxeas (447–519 um), me = spherasters (32 um), mi = sinuous, bifurcated or trifucarted oxyasters (25–30 um), tylasters (9 um)	Siriba Island, Abrolhos Archipelago, Brazil	MNRJ 5316	intertidal	Ribeiro & Muricy, 2004
Tethya brasiliana	Spherical or semispherical, surface tuberculate, stalked buds, cortex 0.75–2 mm	0.7–2.5 cm	Green or yellow externally (*in vivo*), yellow internally	Megasclere bundles with terminal fans, branched up to 5 brushes, rare lacunae	Ms = strongyloxeas (852 um), accessory strongyloxeas (430 um), me = spherasters bifurcate rays (13–84 um), mi = strongylasters = 10 um), microspherasters (10 um), microoxyasters (10 um)	Redonda Island, Abrolhos Archipelago, Brazil	UFRJPOR 4670 A	intertidal	Ribeiro & Muricy, 2004
Tethya cyanae	Hemispherical, tuberculate surface, buds, cortex 0.9–1 mm	1.4 cm	Dark blue externally	Megasclere bundles (100–150 um) with terminal fans, irregular cavities, collagen layer	Ms = strongyloxeas (1026 um), accessory strongyloxeas (532 um), me = spherasters (30 um),	Siriba Island, Abrolhos Archipelago, Brazil	MNRJ 6723	1 m	Ribeiro & Muricy, 2004

(*Continued*)

Table 2. Continued.

Species	External appearance/ attachment	Body diameter	Colour	Skeletal arrangement	Spicules	Type locality	Material	Depth (m)	Reference
				between cortex and choanosome, exogenous particles in the choanosome	mi = oxyasters (26 um), microoxyasters (7.5 um), tylasters (8 um)				
Tethya ignis	Hemispherical, smooth or tuberculate surface, buds, cortex 1–2 mm	1.5 cm	Orange (*in vivo*)	Megasclere bundles projecting beyond the surface, regular cavities, spherasters in the cortex	Ms = strongyloxeas (816 um), accessory strongyloxeas (432 um), me = spherasters (53 um), mi = microspined oxyasters (25 um), tylasters (13 um)	Redonda Island, Abrolhos Archipelago, Brazil	MNRJ 5322a	intertidal	Ribeiro & Muricy, 2004
Tethya maza	Spherical to semispherical, tuberculate surface separated by reticulate areas, buds, cortex 0.125–1 mm	0.6–3.8 cm	Yellow, white or orange (*in vivo*), beige or pinkish in ethanol	Bundles of megascleres, intracortical lacunae, abundant tylasters, spherasters in the cortex	Ms = strongyloxeas (1196 um), me = spherasters (51 um, 18–23 rays), mi = strongylasters type 1 (20 um, 6–9 rays), tylasters type 1 (11 um, 6–8 rays), oxyasters type 1 (11 um, 7–11 rays), oxyasters type 2 (10 um, 6–7 rays)	Urca Beach, Guanabara Bay, Brazil	MNRJ 810		Ribeiro & Muricy, 2011
Tethya beatrizae	Subspherical, smooth, cortex 0.125–2.125 mm thick without lacunae	1.1 cm	Yellow or whitish green (*in vivo*)	Strongylasters and spherasters in the cortex, bundles of megascleres (125–300 um) with terminal fans (500–875 um) project beyond surface, exogenous particles in cortex	Ms = strongyloxeas (948 um), accessory strongyloxeas (414 um), me = spherasters (42 um, 15–20 rays), mi = strongylasters type 2 (12 um, 10–12 rays), oxyasters type 1 (12 um, 8 rays), oxyasters type 2 (8 um, 10–12 rays)	Fernando de Noronha Archipelago, Brazil	MNRJ 7802	1 m	Ribeiro & Muricy, 2011
Tethya nicolae	Spherical, flattened tubercles, cortex 0.1–0.5 mm	1.5 cm	White (in ethanol)	Megasclere tracts protruding beyond surface, ovoid lacunae, cortex with spherasters and oxyasters	Ms = strongyloxeas (1187 um), accessory strongyloxeas (713 um), me = spherasters (48 um, 12–20 rays), mi = strongylasters (13 um, 9–11 rays), tylasters type 2 (11 um, 6–8 rays), oxyasters type 2 (12 um, 10 rays)	Pitimbu–Calypso expedition, Station 1	MNHN.LBIM.D. NBE.1030	45 m	Ribeiro & Muricy, 2011
Tethya solangeae	Hemispherical, microhispid surface, with buds and tubercles, cortex 825–2125 um	2.5 cm	Yellow	Bundles of megascleres almost cylindrical, not fanning out, sometimes forming the tubercles, cylindrical cavities	Ms = strongyloxeas (1238 um), hastate strongyloxeas (414 um), me = spherasters (46 um), mi = strongylasters type II with 10–13 rays (12 um), oxyasters type II with 12 smooth rays (10 um)	Pernambuco state	MNRJ 1488	0.2 m	Ribeiro & Muricy, 2011
Tethya parvula		<1 cm	Yellow				MNRJ 96	3 m	

(*Continued*)

Table 2. Continued.

Species	External appearance/ attachment	Body diameter	Colour	Skeletal arrangement	Spicules	Type locality	Material	Depth (m)	Reference
	Hemispherical, hispid surface, small buds, penducles and tubercles, resistant cortex (1500 um)			Bundles of megascleres (100–150 um), cortical lacunae absent	Ms = strongyloxeas (818 um), hastate strongyloxeas (400 um), me = spherasters with 16–20 conical curved rays (37 um), mi = strongylasters type 2 with 11–18 rays (11 um), oxyasters type 2 with 10–12 smooth rays (9 um), oxyasters type 3 with 10–12 spined rays (13 um)	São Sebastião, São Paulo			Ribeiro & Muricy, 2011
Tethya irregularis	Spherical or subspherical, surface with very small regular cylindric papillae, cortex 0.5 mm in thickness	4.4 mm	White (dry)	Bundles of strongyloxeas compact with slight subdivision in the apical tract	Ms = strongyloxeas (250–1150), not clearly distinct into two categories, me = spherasters and oxyspherasters (50–80 um, R/C 0.2–1.5), in the choanosome also 30 um, 12–14 rays, many with abnormal rays, bent, shortened, or reduced to hemispherical outgrowths; mi = tylasters 10–15 um, with a developed centre, 12–14 slender rays ending in a small knob, similar in the cortex and in the choanosome	Lanzarote, Canary Islands	ZMA 1, ZMA 2–4		Sarà & Bavestrello, 1998
Tethya gracilis	Spherical to subspherical, compressible, flattened tubercles, buds, cortex 1.25 mm, lacunar in the outer zone. Lateral stolons	0.6–1.2 cm	White (live and in ethanol)	Radial bundles, 250 um, fanning and with fascicles. Megasters in 1–2 layers, separated by tissue zone, absent in choanosome, some small megasters upper in choanosome.	Ms = strongyloxeas often a little curved (900–1800 um × 11–15 um), auxiliary strongyloxeas (275–950 um × 2–5 um), me = spherasters (15–45 um, 16–18 rays), tylasters (6–10 um, 3–6 rays, often tetraradiate or few anomalous with forked or distorted rays), strongylasters and oxyasters (10–20 um, 6–8 slender rays), sometimes forked, distorted or with bifid tips	Aquarium of the Aquazoo Löbekke-Museum Düsseldorf	MSNG 50687	Aquaria	Sarà et al., 2001
Tethya aurantium	Spherical, flattened tubercles, one oscule sometimes visible, thick cortex	1–5 cm	Orange (*in vivo*)	Radial bundles not forked, spherasters miltilayered in cortex, interstitial megascleres in between bundles.	Ms = strongyloxeas (400–2500 um × 5–30 um), me = spherasters (50–80 um), mi = tylasters (10–15 um, 9–14 rays), strongylasters (10–15 um, 9–14 rays), and slender oxyasters (15–25 um, 12–14 rays)	Bay of Naples, Italy	MSNG 49670	Littoral	Sarà, 2002

(*Continued*)

Table 2. Continued.

Species	External appearance/ attachment	Body diameter	Colour	Skeletal arrangement	Spicules	Type locality	Material	Depth (m)	Reference
Tethya meloni	Spherical, flattened or scarcely prominent tubercles, one large osculum, thick cortex (0.3–0.5 cm) and may be 1/3 of sponge diameter. Thick collagenous layer	2.9–7.6 cm (5.2 cm)	Cream to pale yellow outside and green-brown inside	Radial bundles wider at cortex, megasters evenly and densely distributed in cortex, scattered in choanosome; micrasters in a thin external cortical layer and also scattered in choanosome	Ms = large strongyloxeas (730–1890 um × 10–40 um, mean 1310 × 25 um), auxiliary strongyloxeas (340–840 um × 8–10 um, mean 590 × 9 um), me = oxyspherasters slightly curved or bifurcated (65.7–119 um, 12–16 rays), R/C = 1–1.8 (mean 1.4), mi = chiasters-tylasters and oxyasters (12–16 um, 8–11 rays), smaller in cortex (13.7–14.9 um, mean 14 um), larger in choanosome (15–17.4 um, mean 16 um), small spines usually at tips	Mar Piccolo di Taranto, SW Apulia, Italy	Museum of Zoology, Bari University, no reg. number	1–120 m, rocky shores, seagrass, deep sea coral gardens (Tuscany Archipelago)	Corriero et al., 2015
Tethya citrina	Spherical, smooth or conulose surface, thin cortex (1–1.5 mm, mean 1.2 mm), thin collagenous layer	0.5–2.6 cm (1.5 cm)	Yellowish or greenish	Radial bundles, wider at cortex, not forked, spherasters monolayered in cortex	Ms = strongyloxea (235–1400 um × 7.5–24 um), me = oxyspherasters (18–64.8 um, mean 42.9 um, 10–20 rays, mean 15), R/C= 0.8–1.4 mean 1.1, mi = oxyaster, chiaster to tylaster (10–15 um, mean 12 um)	Stella di Mare, Adriatic Sea, Italy	Museum of Zoology, Bari University, SDM 1	0–3 m	Sarà & Melone, 1965
Tethya hibernica	Spherical, surface conulose to papillose, tubercles may have stalked buds, cortex compact (0.8–1.4 mm) relatively few lacunae	0.5–2.5 cm	Ochreous-yellow to yellow. In ethanol, white with greyish core	Radial bundles, dense, forming termal fans, megasters evenly and densely scattered in the cortex, micrasters form a discrete layer at exopinacoderm surface and endopinacoderm of lacunae, equally distributed in cortex and choanosome	Ms = strongyloxea (880–1250 um × 8–18 um), auxiliary strongyloxeas (365–820 um × 7–14 um), me = oxyspherasters (31–60 um, 13–18 rays), R/C = 0.4–0.78, mi = oxyspherasters (10–19 um, 10–13 rays), strongylasters (8–18 um, 11–14 rays), tylaster (8–10 um, 7–9 rays) slightly spinulated rays	Rathlin Island, Northern Ireland	Mc3037	Infralittoral to 30 m	Heim et al., 2007
Tethya norvegica	Spherical, contiguous and conulose papillae, consistency resilient, some specimens with	1–2 cm	Ochreous-yellow	Radial bundles, spirally arranged, dense, terminating in a cortical papilla surrounded by a small fan of slender styles. Megasters in outer	MS = strongyloxeas (1200–1500 × 20 um) subtylostyles, auxiliary slender styles (500–700 um × 5–10 um,), me = spherasters (20–60 um, usually 30–50 um, 15	Norway	Syntypes BMNH 1877.5.21.152 and BMNH 1877.5.21.157	10–800 m	Sarà et al., 1992

(*Continued*)

Table 2. Continued.

Species	External appearance/ attachment	Body diameter	Colour	Skeletal arrangement	Spicules	Type locality	Material	Depth (m)	Reference	
	pedunculate buds 1–2 mm diameter, cortex thin (1 mm)			layer of cortex, sparse and irregular distribution. Micrasters in a dense sheet under surface, but also in choanosome, slightly smaller more abundant in cortex	rays) with spines, divided ends and other irregularities, R/C = 0.8–1, mi = oxyasters and rare strongylasters (6–15 um, mainly 8–12 um, 8–12 rays), smooth rays and occasionally developed centre					
Somali/Arabian										
***Tethya orioni* sp. nov.**	Spherical with irregular tubercles, cortex (1.3 mm)	2.7 cm	White in ethanol	Radial bundles of strongyloxeas, 280–400 um thick, form fan-shaped expansions of the cortex, generally subdivided into 3–4 fascicles	Ms = strongyloxeas (1349 um), medium strongyloxeas (856 um), small strongyloxeas (466 um), me = spherasters of 2 sizes (53 and 29 um), mi = strongylasters with 7 spined rays (27 um), oxyasters with 6 spined rays (32 um), tylasters with 9 crown spined rays (13 um)	Abu Dhabi, Persian Gulf	NHMUK 2000.9.14.16		This study	
Tethya omanensis	Spherical or subspherical, smooth with flattened tubercles, cortex 1 mm thick	1–1.5 cm	White in ethanol	Radiating megasclere bundles, spirally arranged, branching in the tubercles	Ms = strongyloxeas/ anisostrongyles (450–980 um), me = spherasters (25–50 um), mi = strongylasters, chiasters, oxyasters, tylasters (10–15 um)	Tiwi Sink Hole, Oman	MSNG 48598	3–9 m	Sarà & Bavestrello, 1995	
Tethya robusta	Subspherical, smooth with depressed tubercles	2–5 cm	Light grey (dried)	Multispiculous fascicles, closely compacted, expanding at the distal apices to tubercles	Ms = strongyloxeas (800–900 um), me = spherasters (60 um), mi = strongylasters (10 um), oxyasters (7 um)	Australia	BMNH			
Tethya seychellensis (Mahe)	Spherical	2.5 cm	Brown	Thick bundles of macroscleres	Ms = strongyloxeas (1000 um), me = spherasters, two sizes (20 and 50 um), mi = strongylasters (10 um), oxyasters (40 um)	Mahé	BMNH		Wright, 1879 (measures from present study)	Supplemental Fig. S4
Tethya seychellensis (Sealark)	Subspherical, tessellated, pore-grooves, cortex lacunar	2.5 cm	Grey-yellow (ethanol)	Thick bundles of macroscleres radiating in stout widely separated fascicles penetrating the cortex	Ms = styles and strongyloxeas, me = two types of spherasters (70 um), oxyasters (40 um, 6 rays), tylasters type 1 (12 um, 6 rays)	Praslin Reef, Salomon Islands	BMNH	20–25 m	Dendy, 1916	
Tethya stellagrandis (Sealark)	Irregularly spherical, tessellated, cortex 0.7 mm	2.5 cm	Grey-yellow (ethanol)	Thick bundles of macroscleres radiating in stout widely separated fascicles penetrating the cortex	Ms = styles and strongyloxeas (1900 um), me = spherasters (250 um), mi = chiasters (16 um, 10 rays), chiasters with slender rays (16 um)	Amirante, Salomon	BMNH	73 m	Dendy, 1916	Supplemental Fig. S5
Tethya ingalli (Sealark)	Subspherical, strongly tessellated in polygonal areas, root-like processes of attachment, cortex 3–4 mm	2.5 cm	Yellowish grey (ethanol)	Spicule bundles penetrate the cortex and spread out into brushes	Ms = strongyloxeas, me = spherasters (80–140 um) R/C = 0.5, mi = cortical tylasters (12–16 um), choanosomal tylaster, strongylaster, oxyasters with short rays (12–20 um)	Praslin Reef, Coetivy, Egmont reef, Salomon Islands	BMNH	18–25 m	Dendy, 1916	

(*Continued*)

Table 2. Continued.

Species	External appearance/ attachment	Body diameter	Colour	Skeletal arrangement	Spicules	Type locality	Material	Depth (m)	Reference
Tethya ingalli	Spherical	–	White	–	Ms = strongyloxeas, me = spherasters (55 um), mi = tylasters (13 um), oxyasters with 6 rays (5 um)	Djibouti, Messageries Reef	–	–	Topsent, 1906
Tethya robusta (previously known as *Donatia arabica*)	Spherical with tubercles, thick cortex, lacunar (not always)	–	Pink, orange	–	Ms = strongyloxeas (1000 um), tylotes, me = two types of spherasters (75 um and 15 um), mi = tylasters and few oxyasters (30 um)	Bay of Djibouti	–	–	Topsent, 1906

Abbreviations: Megasclere tracts (diameter in µm). Ms, megascleres; me, megasters; mi,micrasters (average size in µm).

Fig. 2. *Tethya simoni* sp. nov. MCZ:IZ:133701. A. Field image of a live specimen. B. Skeletal architecture of cortex and upper choanosome in cross section. C. Spherasters, large (with bent tips) and small-size classes. D. Common spherasters with bifurcated tips. E. Strongylaster type 1. F. Strongylaster type 2. G. Oxyaster type 1. H. Tylaster type 1.

Etymology. The species is named after Martin Taboada, the firstborn son of Ana Riesgo.

Tethya simoni Santodomingo, Zea & Riesgo, sp. nov.
ZooBank registration:
urn:lsid:zoobank.org:act:D9D59AFD-4D20-44C0-8737-6243542CD6B5
Fig. 2

Examined material. Holotype: MCZ:IZ:133701 (ex. DNA106631), Bahía de los Delfines (9.21685, −82.21370), Isla Cristóbal, Bocas del Toro, Panama, 15 Mar 2010, leg. A. Riesgo & G. Giribet, 5 m deep. Paratypes: MCZ:IZ:135212 (spec. 3 and 4), same locality as holotype, leg. G. Giribet, 13 Mar 2012; UFBAPOR 5019, UFBAPOR 5020, UFBAPOR 5021, Intertidal rocks on an arenitic plateau at Praia da Pituba, Salvador de Bahia, Brazil, 25 Jan 2018, leg. E. Lanna & F. Calvacanti.

Diagnosis. *Tethya* with thick cortex, spherasters present, in two sizes; larger spherasters often with bifurcated tips, three types of microscleres: strongylasters = tylasters ≪ oxyasters.

Description. Body hemispherical to spherical 0.8–1.2 cm in diameter by 0.9–1.2 cm high (Fig. 2A). Live specimens orange (Fig. 2A), becoming yellow or beige in ethanol. Pinacoderm covered by flattened, circular, irregularly distributed tubercles of variable sizes, 0.2–0.6 mm in diameter with a fiddle-shaped peduncle 0.4–0.7 mm high, separated by reticulate areas. In paratype specimens from Brazil, no tubercles were observed. No oscules evident on holotype nor paratypes.

Skeleton. Cortex 1–1.4 mm thick, with regular lacunae, mainly constituted by abundant spherasters and a thin, outer layer of tylasters. Deposits of collagen form a dense layer between the cortex and choanosome. Main radial bundles of strongyloxeas, 150–250 µm thick, form fan-shaped expansions of the cortex, single or subdivided in 2–3 fascicles. Tylasters present in both choanosome and cortex. Strongylasters and oxyasters more abundant in choanosome.

Spicules. Holotype. Megascleres, strongyloxeas, and spherasters. Main strongyloxeas with rounded and hastate ends, straight, 810.2-1107.5-1470.5 µm long by 9.2-19.3-30.3 µm wide; accessory strongyloxeas with rounded and hastate ends, 210.9-480.3-600.5 µm long by 2.6-9.9-18.4 µm wide (Supplemental Fig. S1B). Spherasters in two sizes, large spherasters more abundant, 72.1-89.5-110.1 µm in diameter, large core 33.3-42.9-53.2 µm, R/C 0.4-0.6-0-7, with 20-22-26 smooth, conical rays, although mainly with variable shapes, more commonly with bifurcated rays (47%), mammilated (20%), or rays with bent tips (20%) (Fig. 2C–D); small spherasters sparse in the cortex with 22-24-26 smooth, conical, straight rays, 45.1-55.9-62.9 µm in diameter, large core 20.5-30.7-35.6 µm, R/C 0.3-0.4-0.6 (Fig. 2C). Microscleres, tylasters, and strongylasters of similar size, larger oxyasters. Strongylasters 11.8-14.7-17.7 µm in diameter, with small nucleus 3.2-4.0-4.6 µm in diameter, and 14-15-16 straight, cylindrical rays with rounded ends, bearing a crown of high, sharp spines, rarely with sparse 1–2 spines at 1/3 to 1/4 of distal portion of rays; rays 4.2-5.6-7.2 µm long by 1.1-1.5-1.9 µm wide (Fig. 2E–F). Tylasters 10.3-12.5-13.9 µm in diameter, with large nucleus 3.4-4.6-5.4 µm, and 12-14-15 straight, short, cylindrical rays enlarged at the tips; short, robust rays 3.7-4.6-5.5 µm long by 1.7-2.0-2.3 µm wide, with large, sharp spines concentrated at the 1/4 ends, mostly pointing upwards; some rays bearing a small spine at their basal part (Fig. 2H). Large oxyasters 18.5-21.7-27.9 µm in diameter, reduced nucleus 4.0-4.5-5.7 µm, and long, straight, thin 12-16-19 rays; rays 7.1-8.4-10.6 µm long by 1.3-1.6-2.0 wide, bearing short, blunt or acerate spines, sparse 1/2 towards the tips, in more density at the 1/4 ends of the rays (Fig. 2G); some oxyasters with bifurcated rays at the 1/3 proximal part.

Distribution and ecology. *Tethya simoni* sp. nov. inhabits the coral reefs of Bocas del Toro (Panama), where it has been found attached to fragments of dead branches of *Porites porites* and other hard corals, around 5 m depth. In Brazil, it was collected under rocks in an intertidal arenitic plateau. This new species is distributed from the southern Caribbean (Panama) to the northeast coast of Brazil.

Remarks. Reports of *T. aurantium* from the Caribbean date back to 1936 in a study of the sponges on both sides of the Panama Canal (de Laubenfels, 1936). Subsequent records include specimens from Puerto Rico and the Dominican Republic (Sarà & Gaino, 1987), from Cuba (Alcolado, 1985), and it is also in a recent checklist from Panama (STRI Research Portal, 2023). These records and some others could be attributed to *T. simoni* sp. nov. (see below). *Tethya aurantium* was described from the Mediterranean Sea, and although we did not have access to the neotype (MSNG 49670, Bay of Naples), *T. aurantium* material studied here was collected in the Bay of Naples. Measurements of our *T. aurantium* specimens from the Mediterranean show a wider and continuous range of strongyloxea size (544.5-1423.2-2366.3 µm long by 11.8-20.8-29.5 µm wide) as well as spheraster size (24.3-76.7-105.1 µm in diameter), which correspond to the neotype description (Sarà, 2002; Table 2). In *T. simoni* sp. nov., strongyloxeas have smaller sizes, and spherasters with bifurcated rays are common, contrary to a unique instance observed in this study on specimen MCZ:IZ:106628 of *T. aurantium* collected in the type locality, in Naples, Italy (Tables 1–2). De Laubenfels (1936) noticed the similarities between his Panamanian specimens and those of *T.*

aurantium from the Mediterranean but remarked the presence of two sizes of spherasters, which are not described for *T. aurantium* but are diagnostic for *T. simoni* sp. nov. (Fig. 2C, Table 2). The molecular affinity of *T. aurantium* and *T. simoni* sp. nov. is clear, as they are sister species in a well-supported clade using two different markers (Figs 3 and 4) and their dominant haplotypes are separated by 8 mutational steps (Fig. 3).

Tethya simoni sp. nov. is constrained to the West Atlantic, and so far only found in the southern Caribbean (Panama) and northeast Brazil. Other examined specimens of the NHMUK collections from the Caribbean and closeby areas (Table 2), included the type of *T. diploderma* NHMUK 1870.5.393 (West Antilles) (Supplemental Fig. S2), USNM 22203 (Panama) and NHMUK 1938.4.26.14 (Bermuda; Supplemental Fig. S3), *T. actinia* BMNH1948.8.6.48 (Bermuda) and *T. taboga* USNM 22216 (Panama). The most important character separating *T. simoni* sp. nov. from these other Caribbean species is the presence of two sizes of spherasters, the most abundant one much larger than those in the other species (Table 2).

Since *T. simoni* sp. nov. also appears in Brazil, we compared it with recently described species from the coast of Brazil, comprehensively reviewed in Ribeiro and Muricy (2011). *Tethya rubra* Samaai & Gibbons, 2005, *T. cyanae* Ribeiro & Muricy, 2004, and *T. ignis* Ribeiro & Muricy, 2004 lack strongylasters, while those are conspicuous in *T. simoni* sp. nov. Diagnostic characteristics of *T. beatrizae* (previously identified as *T. aurantium* sensu Hechtel, 1976 in Ribeiro & Muricy, 2011), such as having a smooth surface (no tubercles) and oxyasters without spines (oxyaster type 2) differ from those of *T. simoni* sp. nov. The main difference from other Brazilian *Tethya* species is the presence of two types of spherasters, one larger than those present in most other Brazilian species, except for *T. brasiliana* Ribeiro & Muricy, 2004 (Table 2). In this particular case, the character distinguishing *T. brasiliana* and *T. simoni* sp. nov. is the absence of tylasters in *T. brasiliana* (Ribeiro & Muricy, 2004). The Brazilian species, *T. nicolae* Ribeiro & Muricy, 2011 and *T. maza* Selenka, 1879, share some characteristics with *T. simoni* sp. nov. *Tethya nicolae* has also spherasters with bifurcated tips, but of much smaller size (37-48-57 µm) and although strongylasters and tylasters have similar shapes and sizes in both species, oxyasters in *T. nicolae* are smaller with smooth rays, contrasting with the typical spinose and sometimes bifurcated in *T. simoni* sp. nov. In comparison with *T. maza*, which also seems to have a wide range of spherasters that vary from a small size (26 µm)

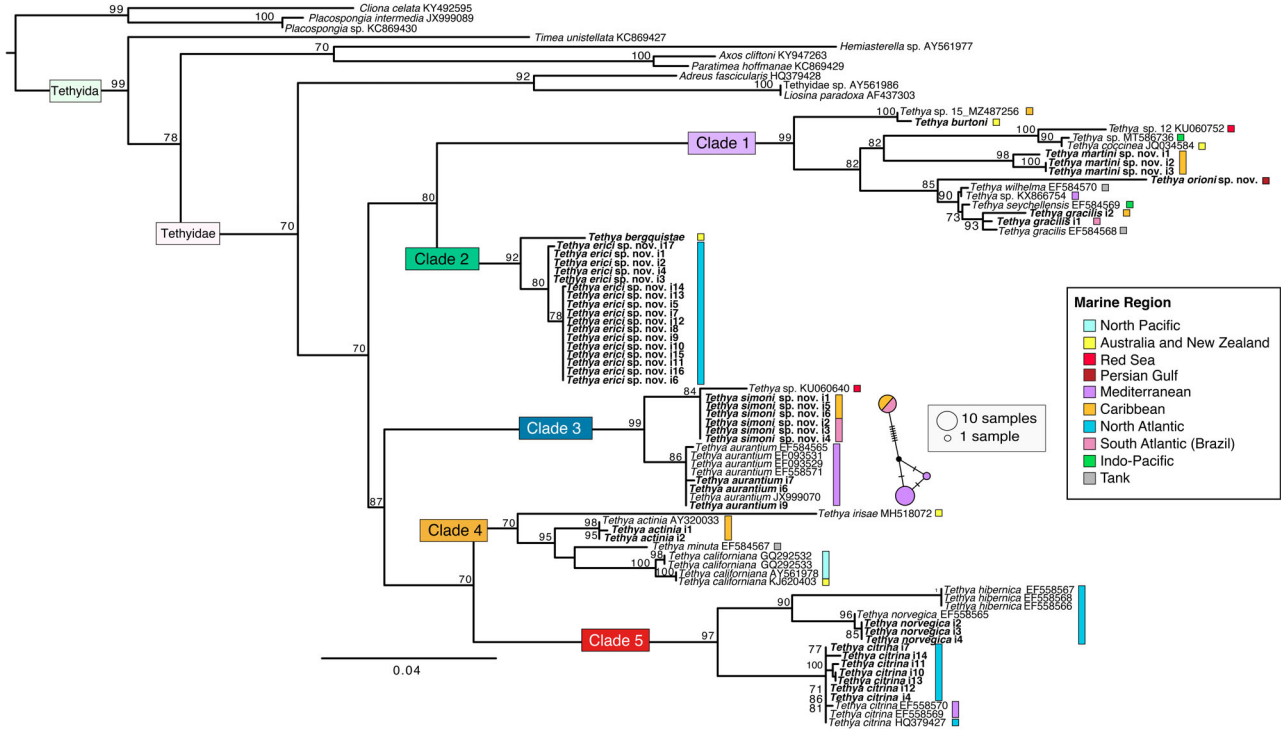

Fig. 3. Maximum likelihood consensus tree for the *cytochrome* c *oxidase subunit I* (COI) alignment. Only bootstrap support values over 70% are shown. In the haplotype network, each circle is a different haplotype for *Tethya aurantium* and *T. simoni* sp. nov., each colour represents a locality, the size of the circle is proportional to that haplotype frequency, and the length of the line is proportional to the number of mutations. Known geographic regions for species in the tree are shown with coloured squares. Specimens in bold letters were sequenced in this study for the first time.

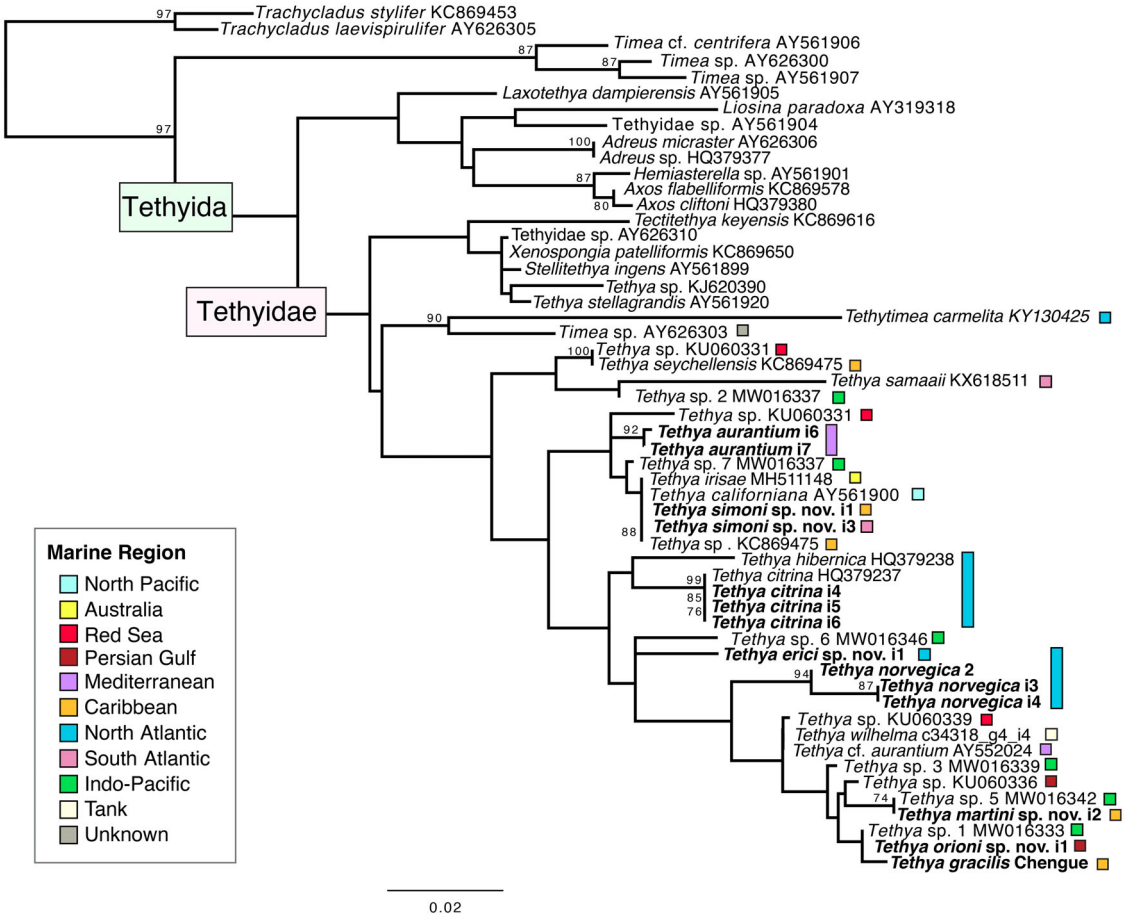

Fig. 4. Maximum likelihood consensus tree for the 28S rRNA alignment. Only bootstrap values over 70% are shown. Known geographic regions for species in the tree are shown with coloured squares. Specimens in bold letters were sequenced in this study for the first time.

to a larger size (100 µm) and some with bifurcated tips, this species has polyrhabds-like spicules (see fig. 1F in Ribeiro & Muricy, 2011, referred to as oxyasters type 1), which are absent in *T. simoni* sp. nov. The wide distribution of *T. maza* along the Brazilian coast, and similarities in the skeletal features, suggest that this species may be part of the same lineage as *T. aurantium* and *T. simoni* sp. nov.

We also compared *Tethya simoni* sp. nov. with specimens collected in the Bay of Chengue (Colombia) (Supplemental Fig. S4) and in Salvador (Brazil) that belong to *T. gracilis* Sarà (Sarà et al., 2001). While *T. gracilis* was described from aquaria in the Düsseldorf Museum for the first time, it is likely that the species originated in a tropical setting that the authors located in the Indo-Pacific based on the affinities of *T. gracilis* to the previously sequenced *T. seychellensis* (see Sarà et al., 2001). However, the sponges could have also originated in the Caribbean. Although the spicular content is similar in both *T. simoni* sp. nov. and *T. gracilis*, *T. simoni* sp. nov. has spherasters of two sizes, with the larger class doubling the size of the ones found in *T. gracilis*, and the strongyloxeas are much smaller in the former species (Table 2).

Etymology. The species is named after the son of Nadia Santodomingo, Simon Peter-Contesse Santodomingo.

Tethya erici Díez-Vives, Santodomingo, Moles, & Riesgo, sp. nov.
ZooBank registration: urn:lsid:zoobank.org:pub:54F80E5E-99A4-43CE-BA3A-BCD01E715595
Fig. 5

Examined material. Holotype: MNCN 1.01/1023, Chipiona 'Corrales', Cádiz, Spain (36.74168, −6.43887). Leg. Juan Moles, 2 m depth, Oct 2014. Paratypes: MNCN 1.01/1024 and MNCN 1.01/1025,

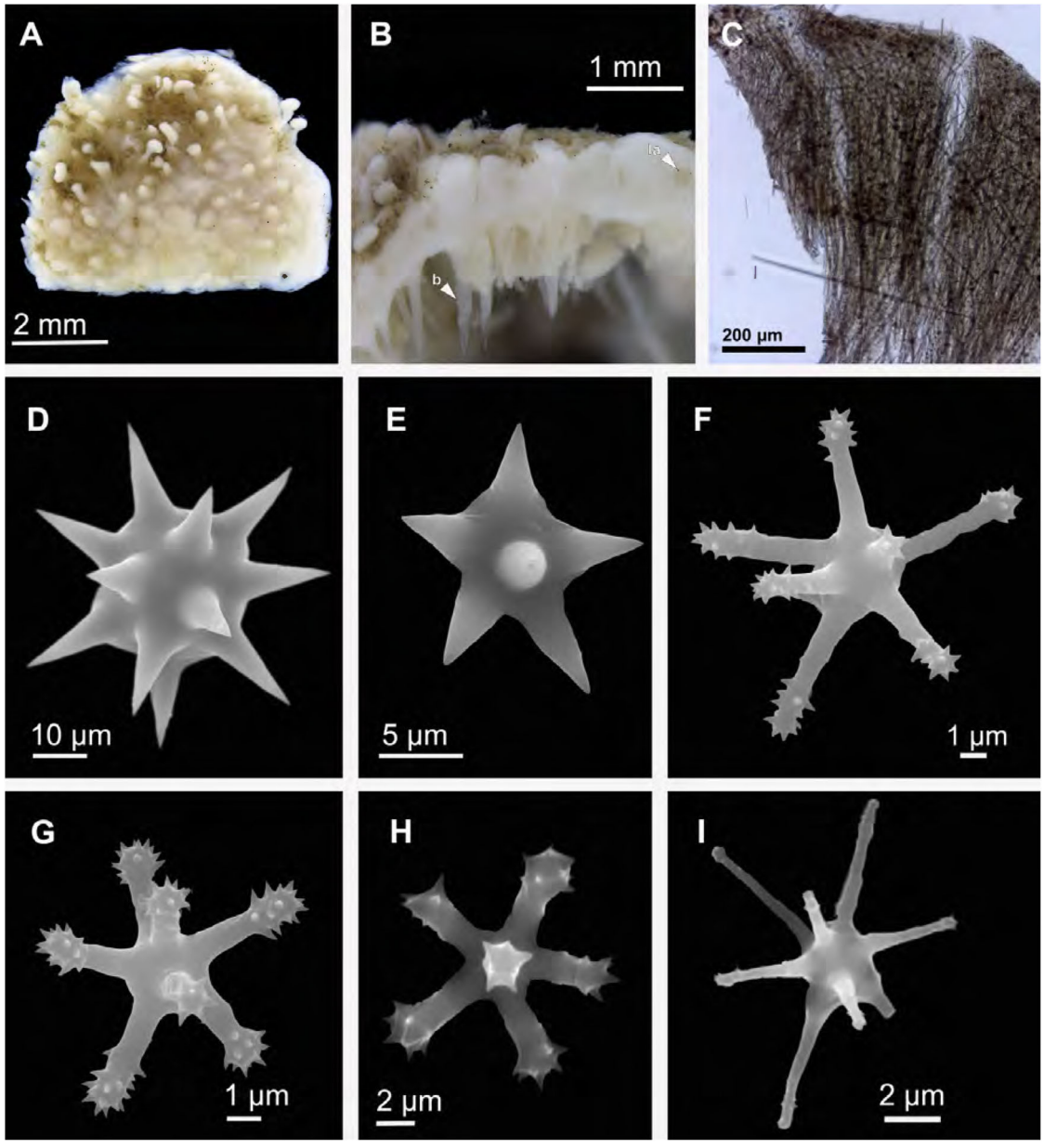

Fig. 5. *Tethya erici* sp. nov. MNCN 1.01/1023. A. Specimen preserved in ethanol. B. Detail of cortex showing bundles (b) and lacunae (la). C. Skeletal architecture. D. Spheraster type 1. E. Spheraster type 2. F. Strongylaster type 1. G. Tylaster type 1. H. Tylaster type 2. I. Oxyaster.

collected with the holotype, and 14 specimens MNCN 1.01/1027 to MNCN 1.01/1041 collected in La Palma, Canary Islands, Spain (28.693245, −17.759086), leg. Juan Moles, 2 m depth, Sept 2022.

Diagnosis. *Tethya* with thin cortex, small strongyloxeas in two sizes, spherasters in two sizes, micrasters: strongylasters, tylasters, and oxyasters, all with similar size ranges, but strongylasters slightly larger and in two types.

Description. Body hemispherical to spherical, 1 cm in diameter; colour green in live specimens, in alcohol white externally, beige internally (Fig. 5A–B). Pinacoderm covered by flattened, plate-like tubercles of variable sizes 0.3–0.4 mm in diameter by 0.1–0.2 mm high, irregularly distributed. Buds with mushroom-like shape, protruding from some tubercles, peduncle 0.4–0.6 mm high and 320–400 µm in diameter (Fig. 5A–B). No oscules evident on holotype nor paratypes. Cortex firm, resistant; choanosome compressible.

Skeleton. Cortex 0.85–0.98 mm thick with regular lacunae (Fig. 5B), mainly formed by abundant spheraster, tylasters, and oxyasters (Fig. 5C). Thin layer of collagen between cortex and choanosome. Main radial bundles of strongyloxeas 250–400 µm thick, forming single fan-shaped expansions of the cortex. Strongylasters mainly present in choanosome, with abundant tylasters and oxyasters, and sparse spheraster (Fig. 5B–C).

Spicules. Holotype. Megascleres, strongyloxeas, and spheraster. Main strongyloxeas with rounded and hastate ends, straight, 808.7-859.1-983.1 µm long by 11.5-14.5-20.4 µm wide; accessory strongyloxeas with rounded and hastate ends, 236.9-340.2-472.86 µm long by 3.6-5.4-7.5 µm wide (Supplemental Fig. S1C). Two sizes of spheraster, small when compared with other *Tethya* species. Spheraster of larger size 15.4-40.1-56.7 µm in diameter, large core 8.2-19.5-25.3 µm, R/C 0.4-0.5-0.7, with 11-13-17 smooth, conical rays (Fig. 5D), and smaller spheraster of 15.2-15.6-16.3 µm, core 6.1-7.1-8.2 µm, R/C 0.5-0.6, with 10–12 conical rays (Fig. 5E). Microscleres, mean size of strongylasters slightly larger than tylasters and oxyasters, but all have similar size range. Strongylasters in two types, 6.9-9.6-11.7 µm in diameter, with small nucleus 1.1-2.6-3.7 µm in diameter, and 7-9-13 straight, cylindrical rays with rounded ends bearing spines at 1/3 to 1/4 of distal portion of rays; strongylaster type 1 have enlarged tips with shorter, sparse spines (Fig. 5F); strongylaster type 2 have conical rounded ends, with sharp and larger spines. Tylasters 5.9-8.3-11.8 µm in diameter, with large nucleus 1.7-2.6-3.7 µm, and 7-8-10 straight, short, cylindrical rays slightly enlarged at the tips; cylindrical rays 1.6-3.1-4.2 µm long by 0.7-1.0-1.1 µm wide, sharp, short spines concentrated at the 1/4 ends, pointing outwards (Fig. 5G–H). Small oxyasters 6.3-8.8-10.8 µm in diameter, reduced nucleus 0.9-1.2-1.6 µm, and long, straight, thin 6-7-9 rays; rays 2.9-3.8-4.4 µm long by 0.3-0.5-0.6 wide, bearing short spines at the 1/4 ends of the rays (Fig. 5I).

Distribution and ecology. *Tethya erici* sp. nov. occurs under rocks on rocky shores in shallow waters (1 m depth), so far only found in the 'Corrales' on the coast of Chipiona (Cadiz, Spain) and La Palma (Canary Islands, Spain) rocky shore pools. The 'Corrales' (Spanish plural of corral) are artificial enclosures historically used for centuries for fishing by hand at low tides. These are rocky enclosures with scattered boulders under which *T. erici* sp. nov. was found. This region is located in the southernmost part of the North Atlantic, near the Strait of Gibraltar, which connects the Atlantic and the Mediterranean Sea. The coast is influenced by the sedimentary inputs of the Guadalquivir River and nearby the large estuarine system of the Doñana National Park. In La Palma, the rocky ecosystems where the sponges were found were mostly intertidal pools under boulders at 2 m depth.

Etymology. The species is named after the son of Cristina Díez-Vives, Eric Nielsen Díez.

Remarks. Among the Atlantic species, *Tethya erici* sp. nov. is most similar to *T. nicoleae* Ribeiro & Muricy, 2011 from Brazil in their spicular content, but the former has smaller strongyloxeas that are in two size classes, spheraster with fewer rays and none with bifurcated tips, microsters of smaller size and more variability with additional strongylasters type 2 and oxyaster type 3. In comparison with other North Atlantic species *T. erici* sp. nov. falls within the range of distribution of *T. aurantium* and *T. citrina*. Although the spicule types are similar to *T. aurantium*, they differ in having smaller sizes, with strongyloxeas and spheraster up to half of the size. Spheraster in *T. erici* sp. nov. have a larger core (R/C 0.4–0.7) different from the typical oxyspheraster (R/C 0.6–1.4) in *T. citrina*. Concerning *T. hibernica* and *T. norvegica*, spicules of *T. erici* sp. nov. are more similar to *T. hibernica* but the latter has typical tylasters of shorter and thicker rays (Heim, Nickel, Picton, & Brümer, 2007). Finally, in contrast to the recently described *T. meloni* Corriero et al., 2015 from the Mediterranean Sea, *T. erici* sp. nov. lacks oxyspheraster (R/C 1–1.8), and tylasters described in *T. meloni* are strongylaster-like with longer rays and smaller cores (Corriero et al., 2015). *T. erici* shares geographic distribution with *Tethya irregularis* Sarà & Bavestrello, 1998 from the Canary Islands, however it differs in the absence of abnormal megasters and the presence of strongylasters and oxyasters. In the molecular phylogeny, *T. erici* sp. nov. forms a well-supported clade with *T. bergquistae* from Australia and New Zealand, which has larger strongyloxeas and microsters (Fig. 3).

Tethya orioni Kenny, Santodomingo & Riesgo, sp. nov.
ZooBank registration: urn:lsid:zoobank.org:act:FB56A581-9311-46EF-A141-8925E0CD58E0
Fig. 6

Examined material. Holotype: NHMUK 2000.9.14.16, tip of causeway, Ras Ghumais, United Arab Emirates, Persian Gulf. Leg. J.D. George, 3–8 m depth, 15 Oct 1998.

Diagnosis. *Tethya* with thick cortex, irregular tubercles, variable spheraster with fewer rays, three types of microsters: oxyasters = strongylasters ≫ tylasters.

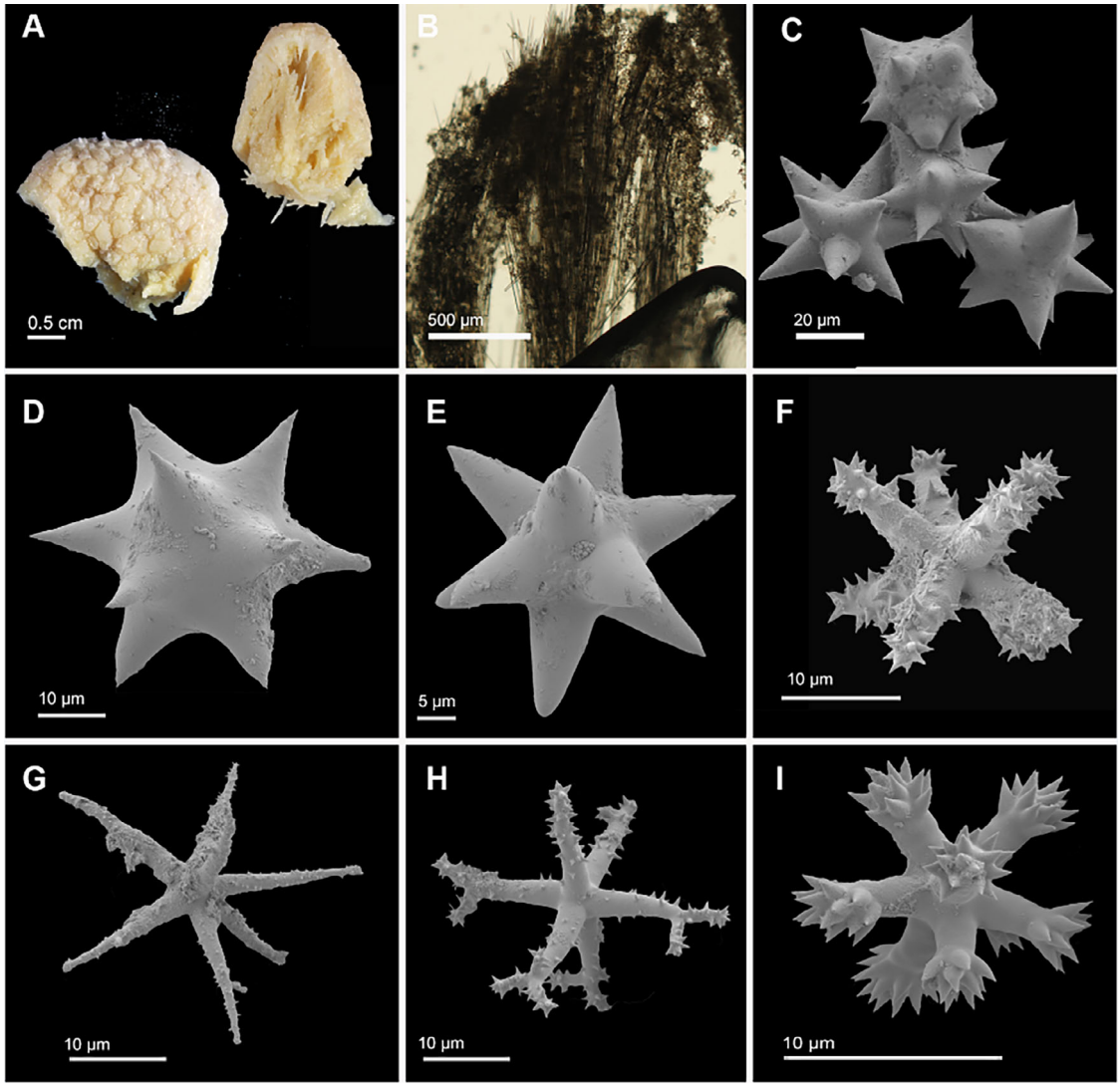

Fig. 6. *Tethya orioni* sp. nov. NHMUK 2000.9.14.16. A. Specimen preserved in ethanol. B. Skeletal architecture of cortex and upper choanosome in cross section. C. Spherasters with abnormal shape and mammillated rays. D. Large spheraster. E. Small spherasters. F. Strongylaster. G. Oxyaster. H. Oxyaster with bifurcated tips. I. Tylaster.

Description. Body spherical 2.7 cm in diameter by 2 cm high (Fig. 6A). Specimen bluish tinge when alive (J.D. George, pers. comm.) and white to light beige in ethanol (Fig. 6A). Pinacoderm covered by tightly arranged tubercles of irregular shape and rugose surface, ranging from 0.5–3.5 mm wide by 0.6–1 mm high. Some buds grow from tubercles, attached through thin peduncles 200–300 µm in diameter and 1.3–2.2 mm long. No oscules visible.

Skeleton. Thick cortex 1–3 mm thick with irregular lacunae, mainly constituted by abundant spherasters and some tylasters (Fig. 6B). Deposits of collagen under the cortex. Main radial bundles of strongyloxeas, 280–400 µm thick, form fan-shaped expansions of the cortex, generally subdivided into 3–4 fascicles (Fig. 6B). Oxyasters and strongylasters abundant in the choanosome. Tylasters less common in choanosome than in the cortex.

Spicules. Holotype. Megascleres, strongyloxeas in three size classes, all straight with rounded and hastate ends. Main strongyloxeas abundant, conform bundles radiating from the centre of the sponge, 1114.3-1349.1-1598.8 µm long by 16.0-20.5-25.7 µm wide (Fig. 5); medium strongyloxeas, less common, 745.1-856.8-956.4 µm long by 10.7-14.8-17.6 µm wide; small, accessory strongyloxeas, profuse, 337.8-466.3-631.0 µm long by 8.0-12.5-16.8 µm wide (Supplemental Fig. S1D). Megasters,

spherasters in two sizes (Fig. 6C–E), large spherasters abundant in the cortex, 40.1-53.3-68.7 µm in diameter, large core 19.9-26.6-32.9 µm, R/C 0.3-0.6-0.9, with 8-13-16 smooth, conical rays (Fig. 6D), but often in irregular and variable shapes, more commonly with unequal rays, both pointy and rounded (20%), thinner rays with mammillae-like tips (15%), or amorphous shape (15%) (Fig. 6C); small spherasters also in variable shapes, sparse in the cortex, more abundant in the choanosome, with 9-11-14 rays, 22.3-29.7-38.1 µm in diameter, core 11.9-15.9-22.7 µm, R/C 0.4-0.6-0.8 (Fig. 6E). Microscleres, strongylasters and oxyasters of similar size, smaller tylasters. Strongylasters 22.0-27.2-35.0 µm in diameter, with small nucleus 5.1-5.8-7.9 µm in diameter, and 6-7-8 straight, cylindrical rays with rounded ends, with sharp spines sparse thoroughly along rays, concentrated towards 1/3 of distal portion of rays; rays 9.9-12.5-16.8 µm long by 1.9-2.5-3.1 µm wide (Fig. 6F). Oxyasters 24.2-32.0-37.3 µm in diameter, reduced nucleus 4.1-5.4-6.4 µm, and long, straight, thin 4-6-8 rays; rays 10.6-15.2-18.5 µm long by 1.6-1.8-2.1 wide, bearing short, acerate spines, sparse thoroughly along the rays (Fig. 6G); most oxyasters with bifurcated rays at the tips (Fig. 6H), some oxyasters devoid of spines with straight rays. Tylasters 10.2-13.3-24.7 µm in diameter, with large nucleus 3.1-4.0-6.6 µm, and 8-9-10 straight, short, cylindrical rays enlarged at the tips, 3.6-5.3-10.4 µm long by 1.2-1.9-2.7 µm wide, with a crown of sharp spines concentrated at the 1/2 ends, mostly pointing upwards (Fig. 6I).

Distribution and ecology. *Tethya orioni* sp. nov. was collected in a sheltered area of a rocky shore, 3–8 m depth.

Remarks. The specimen was deposited in the collections of the NHMUK under the name *T. seychellensis,* identified by Dr Michelle Kelly in 2000. Detailed examination of *T. orioni* sp. nov. in comparison with the *T. seychellensis* holotype NHMUK 1886.10.22.22 (Mahé, Seychelles, Supplemental Fig. S5), showed that both species have similar body size and, despite having densely packed tubercles on the pinacoderm surface, these seem to be more regular in *T. seychellensis*, while very irregular in size and shape in *T. orioni* sp. nov. Spherasters and oxyasters are of similar size in *T. seychellensis* (Table 2), whilst in *T. orioni* sp. nov. oxyasters are smaller than spherasters. Another difference is the presence of strongylasters in *T. orioni* sp. nov., which are absent in *T. seychellensis*. These two species share some features such as the size class of strongyloxeas and tylasters, and by having oxyasters with fewer number of rays and bifurcated tips. Molecular analyses showed that both species are part of the same main clade (clade 1; Figs 3–4) but *T. orioni* sp. nov. can be distinguished morphologically and genetically from other *Tethya* species within that clade. The irregular shape of spherasters in *T. orioni* sp. nov. is a character also observed in *T. omanensis* Sarà & Bavestrello, 1995, described from an underwater cave in Oman, and *T. irregularis* described from the Canary Islands in the vicinity of a freshwater spring (Sarà & Bavestrello, 1998). It has been suggested that these abnormalities and eroded spicular surface are adaptations to reduced salinity (Sarà & Bavestrello, 1998). *Tethya orioni* sp. nov. was collected in a marine setting with no evident freshwater input. *Tethya omanensis* has shorter strongyloxeas (450-720-980 µm), microscleres with an enlarged nucleus, and spherasters with a higher number of rays (24–28) in comparison to those in *T. orioni* sp. nov. Regarding *T. irregularis*, microscleres have a larger number of rays (10–15). Other species described from adjacent waters in the Indian Ocean are *T. stellagrandis* (Dendy, 1916) and *T. ingalli* (Bowerbank, 1858). *Tethya stellagrandis* differs from other species in the genus in having the largest spherasters recorded (up to 250 µm) (Supplemental Fig. S6A–C). In *T. ingalli* spherasters range between 80–140 µm (Dendy, 1916), hence they are double the size of the ones found in *T. orioni* sp. nov.

Etymology. The species is named after Orion Tamati Kenny, the firstborn son of Nathan J. Kenny.

Tethya phylogeny

Phylogenetic analyses of the individual COI and 28S rRNA sequences (Figs 3–4) recovered a monophyletic order Tethyida with strong support (Figs 3–4). The family Tethyidae was also recovered as a single clade with support over 70 in the COI tree, and low support in the 28S rRNA tree (Figs 3 and 4). In the COI tree, we obtained five main clades: clades 1–3 and 5 highly supported but clade 4 with less support (Fig. 3). In clade 1 (Fig. 3), we found *T. burtoni* (from New Zealand) diverging earlier, and then *T. martini* sp. nov. (from Panama), as sister species to a well-supported clade composed by *T. coccinea* (from Australia) and two unidentified *Tethya* specimens collected in the Indo-Pacific and the Red Sea (Fig. 3). Finally, the last subclade obtained in clade 1 grouped *T. seychellensis* (from Vietnam), *T. wilhelma*, and *T. gracilis* (both described from German aquaria), and two specimens that we collected in the western Atlantic, one from the Colombian Caribbean and another from Salvador de

Bahia in Brazil that were extremely similar to the *T. gracilis* holotype. The morphology and spicule complement of the *T. gracilis* holotype (Sarà et al., 2001) and our specimen identified as *T.* cf. *gracilis* from the Caribbean locality of Chengue Bay in Colombia were highly similar (Supplemental Fig. S4), despite a 4 bp difference in COI, suggesting that this species may constitute a species complex, or that its potentially invasive nature has allowed it to diverge quickly into different lineages. Clade 2 grouped two species, *T. bergquistae* from Australia and *T. erici* sp. nov. from the North Atlantic. Clade 3 comprised *T. aurantium*, *T. simoni* sp. nov., and an unidentified specimen of *Tethya* from the Red Sea (Fig. 3). All specimens of *T. aurantium* were collected in the Mediterranean, and showed only two haplotypes, with only one mutational step between them (Fig. 3). For *T. simoni* sp. nov., three specimens were collected in Panama and three more in Salvador (Brazil), and all of them showed a single haplotype shared across their distribution range (Fig. 3). Clade 4 is the least supported clade with a bootstrap of 70%, and comprises *T. minuta* Sarà, Sarà, Nickel & Brümmer, 2001, *T. actinia*, *T. californiana*, and *T. irisae* Sorokin et al., 2019. *Tethya californiana* is represented by two haplotypes with a 3 bp difference (Fig. 3). Clade 5 (Fig. 3) comprised the North Atlantic and Mediterranean species *T. citrina*, *T. norvegica*, and *T. hibernica*.

In the 28S rRNA tree, there is a wider coverage of genera within the family Tethyidae thanks to sequences available in GenBank, including species of the genera *Tethytimea*, *Tectitethya*, *Stellitethya*, *Xenospongia*, and *Tethya* which mostly clustered together in an unsupported clade, diverging the closest to the root within Tethyida (Fig. 4). The sister clade to the general *Tethya* clade was composed of *Tethytimea carmelita* Cruz-Barraza, Vega, Ávila & Vázquez-Maldonado, 2017, and an unidentified *Timea* specimen (Fig. 4). The four clades within Tethyidae observed in the COI tree were not recovered with 28S rRNA data, but it is important to note that many species sequenced for COI were not sequenced for 28S rRNA, so these two trees are not directly comparable. Within the genus *Tethya*, generally, the relationships between the species obtained with COI were mirrored with 28S rRNA (Fig. 4), with a few exceptions: *T. hibernica* did not cluster with *T. norvegica* but with *T. citrina* (Fig. 4).

Microbial composition

Diversity descriptors. The microbial communities were studied in 33 samples. The resulting sequencing reads ranged from 38,288 to 155,303, and the average number of unique amplicon sequence variants (ASVs) was $2{,}723 \pm 1382$ per sample (Supplemental Table S1). *Tethya citrina* i11 (Supplemental Table S1) included the highest number of ASVs (5552), while *T. orioni* sp. nov. had the lowest number of ASVs (461). The most abundant ASV had 69,754 reads in *T. actinia* i3, but in general, only around 2% of the ASVs showed more than 500 reads per sample. Diversity (Shannon*H*) of samples was not statistically different for sponge clades in general and in any of the pair-wise comparisons ($p > 0.05$, Supplemental Fig. S7A), but there were differences between some sponge species pairs ($p < 0.05$, Supplemental Table S2). Interestingly, the 'white' morphotype of *T. aurantium* i9 from Naples was the most diverse sample (5.32, Supplemental Table S1), even when compared with other specimens from the same species and the same location. As expected, *T. orioni* sp. nov. showed the lowest diversity (1.42), dominated by one ASV that comprised 71.5% RA and was annotated as *Synechococcus* CC9902 (100% similarity). Despite these differences in diversity, all 33 *Tethya* specimens whose microbiome was investigated here can be considered LMA sponges.

The ordination of samples based on Bray–Curtis dissimilarity (Supplemental Fig. S7B), showed a grouping of samples by clade, except for *T. norvergica* specimens that were distant to the clade centroid. These latter samples were collected in deep-sea environments and may explain why they did not cluster with their designated clade. Pairwise PERMANOVAs revealed differences between all pairs of clades, which was the result of both differences in location and dispersion of Bray–Curtis dissimilarities (Supplemental Table S1).

Microbial taxonomy. The samples analysed contained from 11–19 different microbial phyla (Supplemental Table S2). In all species, the dominant phylum was Proteobacteria (from 23.8–98.5% RA), except for *T. orioni* sp. nov., where Proteobacteria accounted only for 10% RA and Cyanobacteria dominated its microbiome (86.9%). Cyanobacteria were also abundant in *T. gracilis* from Brazil (35%) and *T. martini* sp. nov. (27 and 32.7% RA), but were below 12% in the rest of the samples. The archaeal community reached important relative abundance in the species *T. erici* sp. nov. (up to 13.7%) and *T. citrina* (up to 32.4%) (Supplemental Table S3). Also, samples of *T. erici* sp. nov. presented an unusually high abundance of sequences without a confident taxonomic classification beyond the kingdom Bacteria (up to 38.7%), for both 'la Palma' and 'Chipiona' samples. Since all samples were processed similarly, the reasons for this difference are unclear but could indicate the presence of bacterial taxa that are not well represented in the current databases.

At the deeper level of order, the microbial community of *Tethya simoni* sp. nov. and *T. aurantium* (both comprising clade 3) was mostly formed by Microtrichales (Actinobacteriota), Rhodobacterales (Alphaproteobacteria), UBA10353 marine group (Gammaproteobacteria), and other unclassified Proteobacteria (Supplemental Table S2, Fig. 7A). *Tethya citrina* harboured mostly Burkholderiales (Gammaproteobacteria) and Nitrosopumilales (Crenarchaeota). However, in *T. norvegica*, which also belonged to clade 5, Pirellulales were more abundant (reaching up to 54.4% RA), and Parvibaculares (Alphaproteobacteria, up to 43.9%), while Nitrosopumilales and Burkholderiales were less abundant. The three species belonging to clade 1 were characterized by the dominance of Synechoccales (Cyanobacteria), with some differences in other taxonomic orders such as high abundances of Rhodobacterales (Alphaproteobacteria) in *T. gracilis*, or high abundance of SAR11 clade (Alpaproteobacterias) in *T. martini* sp. nov. Finally, clade 2, represented by *T. erici* sp. nov. in our analysis, presented similar dominant taxonomic orders as the rest of *Tethya* species but with different relative abundances, and particular abundance of Cytophagales (Bacteroidota) (Supplemental Table S2).

The sample clustering based on abundances at ASV level was congruent with the clades of the COI phylogeny (Figs 3 and 7A, Supplemental Fig. S8), although the topology showed small variations in some relationships. For instance, *T. gracilis* clustered with *T. martini* sp. nov., instead of with *T. orioni* sp. nov. in the microbial clustering (Fig. 7A). However, it is important to note here that the relationships within these clusters can slightly differ depending on the taxonomic resolution

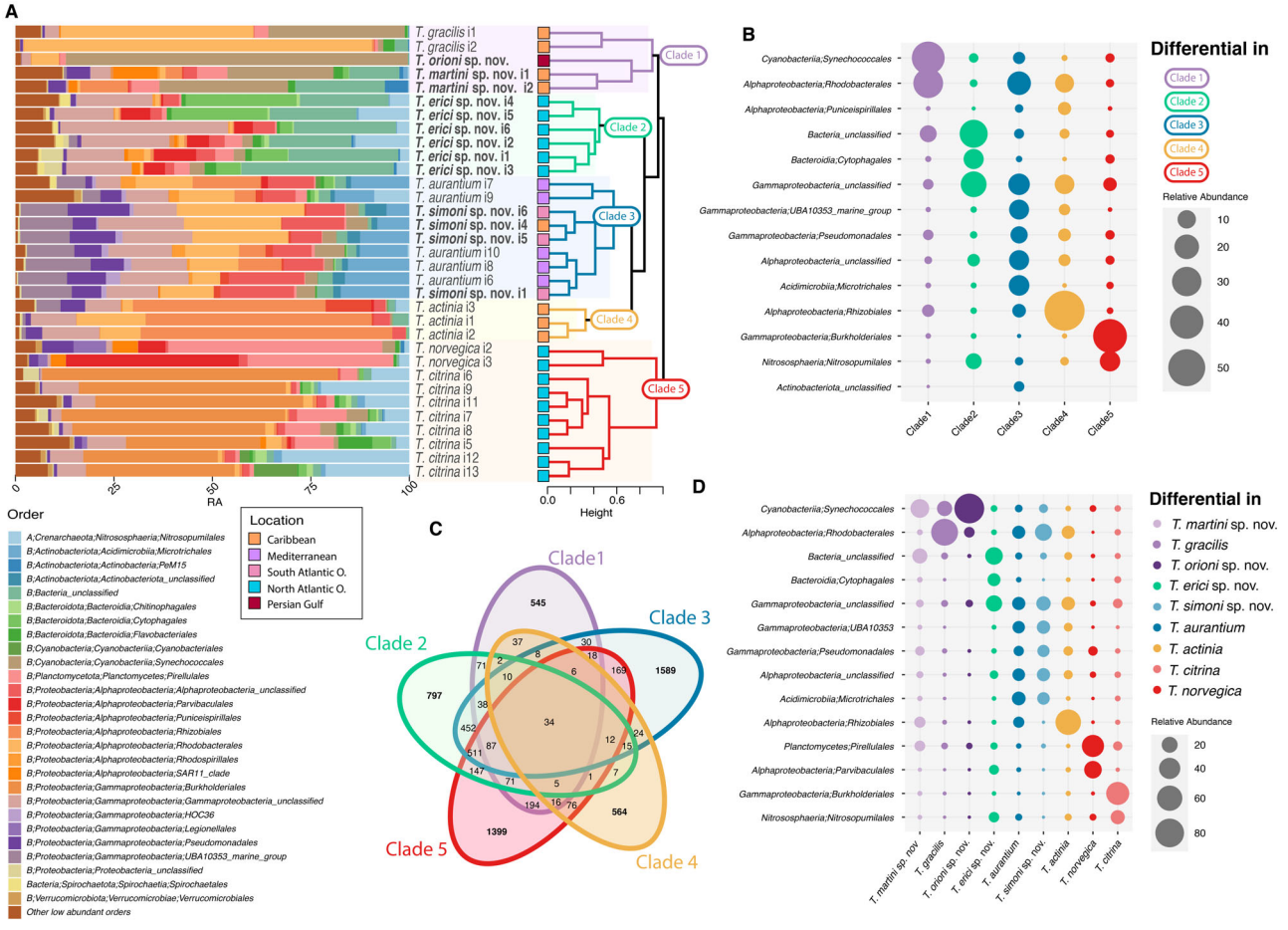

Fig. 7. Microbiome composition for *Tethya* spp. A. Barplot showing the relative abundance of each microbial (Bacteria and Archaea) order with corresponding dendrogram clustering of the samples using Bray–Curtis dissimilarity values. B. Differentially abundant microbial orders between sponge species that represent > 10% RA. Highlighted orders include the ones that are significantly significant in any of the pairwise comparisons (see Supplemental Table S6). C. Venn diagram of shared and unique ASVs for the four clades sequenced. D. Differentially abundant orders that are significant for all pairwise comparisons between one clade and the other three (see Supplemental Table S5). Circles for 'diagnostic' microbial taxa show a black stroke in both B and D.

used for the microbial composition. For example, in a dendrogram based on the genus level abundances, clade 2 branches as a sister group of clade 3, a pattern more similar to the COI tree (Supplemental Fig. S8).

Core microbiome and differentially abundant orders. Only two core ASVs were shared among 70% of the samples: one *Synechococcus* and one *Rubripirellula* (Planctomycetes). This core reached a relative abundance ranging from 0 in *T. norvegica* to 17.8% in *T. gracilis* from Brazil (Supplemental Table S5). In pairwise comparisons, the largest number of shared ASVs occurred intraspecifically in samples of *T. citrina* (up to 1171 ASVs) and *T. erici* sp. nov. individuals (up to 816 ASVs) (Supplemental Table S6).

Across geographic areas, *Tethya simoni* sp. nov. shared 427–624 ASVs in samples from Brazil and Bocas del Toro; *T. citrina* from la Palma, Galicia, and Roscoff shared from 47–463 ASVs; *T. erici* sp. nov. from la Palma shared from 177–503 ASVs with the samples from Chipiona. Across species, *T. erici* sp. nov. shared many ASVs with *T. citrina* samples, with the highest values found among samples of both species collected in the same area (las Palmas) (from 327–726). Interestingly, the *T. aurantium* 'white' phenotype also shared high numbers of ASVs with these *T. erici* sp. nov. and *T. citrina* samples (up to 630 ASVs) (Supplemental Table S1).

Among clades (i.e., considering the mean of all microbial sequences present in any sample belonging to the clade), the core microbiome included 37 ASVs, spanning different phyla (Fig. 7C and Supplemental Table S5), and the specific ASVs of each clade ranged between 545 (11.5% of ASVs in clade 1) to 1589 (15.3% of ASVs in clade 3, Fig. 7C). These exclusive ASVs and other taxonomic orders that differed in abundance in one clade compared with the other four clades can be considered indicator taxa of the clade, and are shown in Fig. 7B. For instance, clade 1 presented larger abundances of Synechococcales in all pairwise comparisons, and Rhodobacterales in the comparison between clades 1 and 5. Clade 2 displayed larger abundances of Cytophagales, and, as commented above, a significant proportion of unclassified bacterial sequences. Clade 3 was characterized by Microtrichales, UBA10353 marine group, Pseudomonadales, and unclassified Alphaproteobacteria. Clade 4 distinctively harboured high proportions of Rhizobiales, and clade 5 of Burkholderiales and Nitrosopumilales. Other microbial taxonomic orders that were statistically distinct in some pairwise comparisons among clades can be found in Supplemental Table S7 and Supplemental Fig. 7C. Furthermore, some taxonomic orders were specific to the sponge species but not the entire clade. This situation is noticeable in clade 5, where Burkholderiales and Nitrosopumilales are representative of *T. citrina*, but Pirellulales and Parvibaculales are characteristic of *T. norvegica* (Fig. 7D). Similarly, Rhodobacterales was abundant in *T. gracilis*, while Synechococcales dominated *T. orioni* sp. nov. (Fig. 7D). Additional orders with less than 10% RA can be found in Supplemental Table S8 and Supplemental Fig. S7D.

Discussion

Phylogeny and biogeography

In this study we describe four new species in the genus *Tethya*, two from the Western Atlantic (southern Caribbean and Brazil), one from the North Atlantic, and one from the Persian Gulf, by integrating morphology, genetics, and their associated microbial communities. We revisited the phylogeny of this group by adding new sequence data from freshly collected material, museum specimens, and unpublished data. Our revised phylogeny retrieved the main clades found in previous studies (Heim et al., 2007; Heim & Nickel, 2010; Sorokin et al., 2019), but incorporated samples representing new biogeographic regions. Interestingly, in our phylogenetic hypothesis, most clades and subclades do not show a clear biogeographic affinity, as they grouped specimens inhabiting disparate regions (Fig. 3). The weak biogeographic concordance uncovered in this study could be explained by an early divergence of Tethyidae and its cosmopolitan genus *Tethya*. According to recent time-calibrated phylogenies, this divergence has been estimated to have occurred during the late Permian/Triassic period (260–210 Ma) (Pankey et al., 2022; Plese et al., 2021), although the only fossil record for *Tethya* is from the Eocene (Łukowiak, 2016). Our results also support the idea of the early radiation in this genus proposed by Sarà and Sarà (2004) but suggest that this may have taken place earlier than previously thought (Heim, Nickel, & Brümmer, 2007). The origin of the main lineages may have occurred in the context of an ancient Palaeo-Tethys fauna (late Permian/Triassic) and subsequent radiation throughout the Mesozoic linked to the break-up of Gondwana. Therefore, the most plausible explanation for the current diversity and distribution of Australian and Caribbean *Tethya* species within the same clades is that they have deep roots and display a relict Tethyan pattern (Heim et al., 2007; Sarà & Sarà, 2004). This hypothesis is further supported by the sympatric occurrence of species belonging to distant evolutionary clades. To the classic example of *T. aurantium* (clade 2) and *T. citrina* (clade 4) from the Mediterranean (Sarà, 1990), we add that the new species

from the southern Caribbean, *T. martini* sp. nov. (clade 1), *T. simoni* sp. nov. (clade 3), and *T. actinia* (clade 4) show also a high genetic distance, belonging to quite divergent clades of COI (Fig. 3).

The early 20th century was pervaded by descriptions of *Tethya* species widely distributed across all oceans, such as *T. aurantium*, *T. diploderma*, or *T. seychellensis*. The cosmopolitanism of these species has been previously refuted (Ribeiro & Muricy, 2011), and our results provide further evidence of this. The extreme similarities in morphology and close molecular affinity of *T. simoni* sp. nov. and *T. aurantium* make them easy to be confused, and thus researchers assigned them to the same species. Our results show, in turn, that the once-thought-widespread *T. aurantium* might be restricted to the Mediterranean Sea or at least the NE Atlantic, as suggested by Heim et al. (2007). These species from both sides of the Atlantic have a high genetic distance (two distinct COI haplotypes with eight mutations, Fig. 3), higher than in other sibling Porifera species (e.g., Cárdenas et al., 2013; Duran & Rützler, 2006).

Another interesting finding in our study is that two specimens from the southern Caribbean and the South Atlantic coast in Brazil were identified morphologically and genetically as *T. gracilis*, a species originally described from German aquaria. Our data also suggest a Western Atlantic origin for this species, refuting an Indo-Pacific origin for *Tethya gracilis*, as previously proposed based on a morphological resemblance to *T. seychellensis* (Sarà et al., 2001) and its grouping within the same genetic clade (Heim, Nickel, & Brümmer, 2007). Establishing the origins of the three species described from German aquaria, *T. wilhelma*, *T. minuta*, and *T. gracilis* (see Sarà et al., 2001), is relevant because of their use in experimental studies on kinetics, functional morphology, and biomechanics in clades of early-branching metazoans (Ellwanger & Nickel, 2006; Nickel et al., 2006). The affinity of *T. minuta* with *T. actinia* described from Bermuda (Heim et al., 2007) tilts the balance towards an Atlantic provenance of two of the species of *Tethya* from aquaria, leaving only *T. wilhelma* as the one possibly coming from the Eastern Mediterranean Sea (Sorokin et al., 2019). Indeed, the sequence from *Tethya* sp. (KX866754), originally identified as *T. aurantium* (see Idan et al., 2018) is strikingly similar to that of *T. wilhelma*, with only 1 bp difference in COI, suggesting that the origin of *T. wilhelma* might be the Eastern Mediterranean or the Red Sea. Since the type localities of the three species are three different public aquaria (Stuttgart, Karlsruhe, and Düsseldorf), it is likely that they may have originated from different geographic regions. Although less probable, an alternative scenario to the Atlantic origin for *T. gracilis* could be its recent introduction from the Indo-Pacific via ballast water or biofouling on ship's hulls (e.g., *Mycale grandis* Shih & Popp, 2020). However, previous records of *T. seychellensis* in the Colombian Caribbean could correspond to *T. gracilis* (e.g. Wintermann-Kilian & Kilian, 1984) and the high diversity of *Tethya* species in Brazil would support that *T. gracilis* is most likely native to these regions.

The addition of species from *Tethya* hotspots such as Australia, Brazil, the Malay Archipelago, and the Galápagos islands in future phylogenetic analyses will bring more insights to the understanding of the evolution of this diverse genus. Although in this study we attempted to include some of the Brazilian species using subsamples from the MNRJ in Brazil, we were unsuccessful in recovering sequences due to low-quality DNA preservation. Further studies may consider the inclusion of museum material through the implementation of mini-barcodes specifically designed to amplify partial COI sequences from degraded DNA (Cárdenas & Moore, 2019) or the use of short-read sequencing technologies, which have proved much more efficient in dealing with degraded museum samples (Derkarabetian et al., 2019; Srivathsan et al., 2021).

Systematics

Taxonomists, systematists, and field ecologists strive for easily observed diagnostic features with high discrimination power. Among the morphological features with the potential to become diagnostic for systematics, colour has been proposed as a reliable character to support some of the clades in *Tethya* (Sorokin et al., 2019). Clades 1 and 2 include red, pink or white species, clade 3 are mainly orange, while clade 4 is composed of mainly yellow species. Our newly described species bring more evidence to this hypothesis, and, as expected, the bright red *T. martini* sp. nov. groups in clade 1 with *T. seychellensis* and *T. coccinea* (all red) and the orange *T. simoni* sp. nov is part of clade 3 with *T. aurantium* (both orange). However, there are some exceptions to these trends. In fact, monitoring studies of *Tethya* spp. in New Zealand have shown that the same sponge can experience variations in shape and colouration depending on seasonal environmental changes (Shaffer et al., 2020). In any case, the colour-based hypothesis in *Tethya* species demands further investigation as this character could be genetically controlled, since it may be related to the presence of carotenoids (Tanaka et al., 1982; Tanaka & Yamamoto, 1984) produced by the sponges (Liaaen-Jensen et al., 1982) or symbionts, unicellular green algae, or Cyanobacteria (Belikov et al., 2019).

The usual morphological diagnostic characters of spicule morphologies in *Tethya* are especially problematic, due to the lack of a homogeneous terminology for the genus. This has been a persistent issue throughout the taxonomic history of *Tethya* (Bergquist & Kelly-Borges, 1991). Therefore, it is important to emphasize that most-needed phylogenetic analyses within this species-rich genus first require the unification of terminology for spicule types based on quantitative morphometric measurements. For instance, an effort to encompass the wide variation of microscleres has resulted in the distinction of three main types, i.e., tylaster, strongylaster, and oxyaster (~previously pooled in chiasters, although most referred to tylasters and strongylasters), and subtypes within (e.g. Ribeiro & Muricy, 2011 used numbers for subtypes, while Hajdu et al., 2013 added the prefix acanthose). Yet their definitions were rather qualitative, leaving room for some intermediate forms of difficult designation. Therefore, the redescription of type material under such a unified morphological framework would facilitate mapping characters onto phylogenetic trees. Finally, identifying new and reliable external characters and from histological sections, e.g., tubercle shape, lacunar structure, and collagenous distribution could help to assign species to their taxonomic units. Although in our study we followed the nomenclature of spicules by Ribeiro and Muricy (2011) to allow comparisons with other Western Atlantic species, we recommend that a comprehensive nomenclature framework should also take into account the definitions proposed by Bergquist and Kelly-Borges (1991), Sarà and Sarà (2004) and Heim, Nickel, and Brümmer (2007), to cover the wide spectra of spicule variation across the different biogeographic regions.

Microbial composition

Integrative taxonomy aims to incorporate several lines of evidence that converge in robust hypotheses for species delimitation. In the field of sponge systematics, integrative taxonomy mainly includes morphological and molecular characters (Dohrmann et al., 2017; Riesgo et al., 2018; Sorokin et al., 2019). In recent years, several authors have tried to also incorporate metabolomics (Reveillaud et al., 2012; Ruiz et al., 2015) and ecological/biogeographic data (e.g., Azevedo et al., 2015). Surprisingly, the microbiome has never been formally used as a taxonomic character, despite its remarkable species-specificity (Thomas et al., 2016) and studies hinting at cophylogeny/coevolution patterns with their hosts (Pankey et al., 2022; Schöttner et al., 2013). Coevolution or phylosymbiotic patterns in marine invertebrates are especially conspicuous in sponges and cnidarians, which harbour complex communities of prokaryotic symbionts (O'Brien et al., 2019). In sponges, the host is usually the factor driving most divergences in the coevolutionary patterns (Thomas et al., 2016), with those being more pronounced at high taxonomic levels, such as order, and less clear in LMA than in HMA sponges (Pankey et al., 2022). Our analysis shows high levels of coevolution in the host and microbial communities of LMA sponges, even within a single genus of sponges. Nonetheless, small discrepancies can be observed at different levels of microbial taxonomy, both in our study and across the literature. Thus, the microbiome emerges as an informative intrageneric diagnostic character with enormous potential for taxonomic identification and evolutionary studies, especially for species in which COI is extremely conserved (for instance Riesgo et al., 2016). In fact, in our study, although the clustering analysis of the prokaryotic communities at ASV level only correlated moderately with the phylogenetic hypothesis obtained with COI (Figs 3 and 7A, Supplemental Fig. S8), the distinctive microbial communities for the different clades suggest that these could be considered an additional taxonomic feature to aid in *Tethya* systematics. This high specificity shown by *Tethya* in their microbial communities was previously proposed by Sipkema and Blanch (2010) as an alternative approach to differentiate between species. Interestingly, once *T. norvegica* was removed from the microbial analysis, the correlation between the clustering analysis of the microbiome and the COI tree improved (Supplemental Fig. S8). In fact, the microbiome of *T. norvegica* was very different from that of the rest of specimens in Clade 5 (*T. citrina*) and from those in other clades, likely because it is a deep-sea species, which typically hosts a distinctive microbiome (Díez-Vives & Riesgo, 2024).

The microbiome of the previously studied species of *Tethya* is dominated by temporally stable Proteobacteria species, usually represented by a single, dominant operational taxonomic unit (OTU or ASV in our case), followed by Cyanobacteria and Bacteroidetes (Astudillo-García et al., 2020; Sipkema & Blanch, 2010; Thiel et al., 2007; Waterworth et al., 2017). Although our results can hardly be compared with these previous studies because the primers used for the amplification of the 16S rRNA gene were different, an overall gross comparison also points to the dominance of Proteobacteria (Fig. 7). These phyla are also typically dominant in other LMA sponges (Moitinho-Silva, Steinert, et al., 2017). In our study, Cyanobacteria were present across all species but dominant in clade 1, with the order Synechococcales distinctive of the group. Interestingly, the microbiome of *T. burtoni*, which belongs to clade 1 (Fig. 3), was sequenced

by other researchers and did not show a dominance of Cyanobacteria (Astudillo-García et al., 2020) but, in this case, the primers used could have had an amplification bias different from ours. Several other microbial taxa were characteristic of each of the clades we recovered. For instance, only *Tethya* species from clade 3 have abundant communities of Actinobacteria (in our case of order Microtrichales), which were also recovered from other *T. aurantium* samples (Thiel et al., 2007) and the species *T. californiana* (Sipkema & Blanch, 2010), which clusters also in clade 3 according to our phylogenetic results. Similarly, an unidentified species of *Tethya* collected on Orpheus Island in Australia had Actinobacteria dominating the community, together with Proteobacteria, Chloroflexi, Crenarchaeota, and Verrucomicrobia (Thomas et al., 2016). However, whether this unidentified species belonged to clade 3 is currently unknown. *Tethya citrina* (clade 5) was remarkably dominated by Burkholderiales (Gammaproteobacteria). This group is hard to track in the literature because it has been reorganized differently in the available databases; it was formerly known as class Betaproteobacteria, but can also be found as an order placed within class Betaproteobacteria, or as class Gammaproteobacteria (i.e., NCBI and SILVA taxonomy) (Parks et al., 2018). Recently, Taylor et al. (2021) characterized this group classifying it as a new gammaproteobacterial order named *Candidatus* Tethybacterales. Only a Metagenome-Annotated Genome (MAG) annotated as *Beroebacter blanensis*, and assembled from *Crambe crambe* (Schmidt, 1862) from the Mediterranean Sea, could be detected among 14 of our samples covering all species (100% sequence identity), although in low abundances (up to 0.007% RA). In summary, although the use of the microbiome as a diagnostic character has only been tentatively explored here, it holds enormous potential for future taxonomic studies, especially in groups where the morphology and the molecular characters are highly homoplastic.

Acknowledgements

We are indebted to J. David George (NHMUK) for details regarding the collection of *Tethya orioni* sp. nov., to Guilherme Muricy (MNRJ/UFRJ) who kindly sent subsamples of *Tethya* types from Brazil for comparison, to Yann Fontana (Roscoff Marine Station) for collecting *T. citrina* and to Jim Drewery (Marine Scotland Science) for collecting *T. norvegica*. We are also thankful to Tom White and Lauren Hughes (NHMUK) for help during specimen deposits and to Gilberto Bergamo for his invaluable assistance in taking photos of the specimens of *T. erici* sp. nov. We thank Miguel Martelo and Catalina Arteaga (Invemar) for allowing us access to the material from Colombia and Fernanda Cavalcanti (UFBA) for helping to collect several specimens from Brazil. We are grateful to Megan Shaffer (Victoria University of Wellington, NZ) for sharing her COI sequences of *T. bergquistae* and *T. burtoni*. We also thank Rob van Soest for fruitful discussions and valuable insights into deciphering the spiky taxonomy of *Tethya*. Two anonymous reviewers provided insightful comments that helped us improve this work.

Supplemental material

Supplemental material for this article can be accessed here: http://dx.doi.org/10.1080/14772000.2024.2383341.

Disclosure statement

No potential conflict of interest was reported by the author(s).

Funding

This study was funded by the Department of Business, Energy, and Industrial Strategy (BEIS) through two Rutherford Fellowships to AR, NS, and EL. JM acknowledges support from the Spanish Government through the HETGEN1000 project [PID2021-127037NA-I00/MCIN/AEI/10.13039/501100011033/and by FEDER una manera de hacer Europa]. This study was further supported by two grants from the Spanish Ministry of Science and Innovation [PID2019-105769GB-I00 and RYC2018-024247-I] and an internal grant from CSIC [PIE-202030E006] to AR. Also, CDV received the support of a fellowship from 'la Caixa' Foundation [ID 100010434], code LCF/BQ/PI22/11910040. NJK was supported by a Rutherford Discovery Fellowship [RDF-UOO2001] from Te Apārangi, The Royal Society of New Zealand. Finally, part of this research was supported through the SponBIODIV project (AR and PC), a 2021–2022 BiodivProtect joint call for research proposals, under the Biodiversa + Partnership co-funded by the European Commission, and with the funding organizations 'Fundación Biodiversidad' and FORMAS.

ORCID

Nadia Santodomingo http://orcid.org/0000-0003-1392-2672
Cristina Díez-Vives http://orcid.org/0000-0002-1772-7092

Nathan J. Kenny http://orcid.org/0000-0003-4816-4103
Paco Cárdenas http://orcid.org/0000-0003-4045-6718
Laura Balcells http://orcid.org/0000-0001-9829-3961
Juan Moles http://orcid.org/0000-0003-4511-4055
Sven Zea http://orcid.org/0000-0002-5657-4877
Gonzalo Giribet http://orcid.org/0000-0002-5467-8429
Emilio Lanna http://orcid.org/0000-0002-6170-1842
Carlota Gracia-Sancha http://orcid.org/0009-0009-7316-1132
Ana Riesgo http://orcid.org/0000-0002-7993-1523

References

Alcolado, P. (1985). Estructura ecológica de las comunidades de esponjas en Punta del Este. *Reporte de Investigación Del Instituto de Oceanología*, 38, 1–66.

Apprill, A., McNally, S., Parsons, R., & Weber, L. (2015). Minor revision to V4 region SSU rRNA 806R gene primer greatly increases detection of SAR11 bacterioplankton. *Aquatic Microbial Ecology*, *75*, 129–137. https://doi.org/10.3354/ame01753

Astudillo-García, C., Bell, J. J., Montoya, J. M., Moitinho-Silva, L., Thomas, T., Webster, N. S., & Taylor, M. W. (2020). Assessing the strength and sensitivity of the core microbiota approach on a highly diverse sponge reef. *Environmental Microbiology*, *22*, 3985–3999. https://doi.org/10.1111/1462-2920.15185

Austin, W. C., Ott, B. S., Reiswig, H. M., Romagosa, P., & McDaniel, N. G. (2014). Taxonomic review of Hadromerida (Porifera, Demospongiae) from British Columbia, Canada, and adjacent waters, with the description of nine new species. *Zootaxa*, *3823*, 1–84. https://doi.org/10.11646/zootaxa.3823.1.1

Azevedo, F., Cóndor-Luján, B., Willenz, P., Hajdu, E., Hooker, Y., & Klautau, M. (2015). Integrative taxonomy of calcareous sponges (subclass Calcinea) from the Peruvian coast: Morphology, molecules, and biogeography. *Zoological Journal of the Linnean Society*, *173*, 787–817. https://doi.org/10.1111/zoj.12213

Belikov, S., Belkova, N., Butina, T., Chernogor, L., Martynova-Van Kley, A., Nalian, A., Rorex, C., Khanaev, I., Maikova, O., & Feranchuk, S. (2019). Diversity and shifts of the bacterial community associated with Baikal sponge mass mortalities. Public Library of Science *One*, *14*, e0213926. https://doi.org/10.1371/journal.pone.0213926

Bergquist, P. R., & Kelly-Borges, M. (1991). An evaluation of the genus *Tethya* (Porifera: Demospongiae: Hadromerida) with descriptions of new species from the Southwest Pacific. The Beagle, Records of the Museums and Art Galleries of the Northern Territory. *Museum of Arts and Science*, *8*, 37–72.

Boury-Esnault, N., & Rützler, K. (Eds) (1997). Thesaurus of sponge morphology. *Smithsonian Contributions to Zoology*, *596*, 1–55. https://doi.org/10.5479/si.00810282.596

Bowerbank, J. S. (1858). XVI. On the anatomy and physiology of the spongiadæ. *Philosophical Transactions of the Royal Society of London*, 279–332.

Brusca, R. C., Giribet, G., & Moore, W. (2023). *Invertebrates* (4th ed.). Oxford University Press.

Callahan, B. J., McMurdie, P. J., & Holmes, S. P. (2017). Exact sequence variants should replace operational taxonomic units in marker-gene data analysis. *The ISME Journal*, *11*, 2639–2643. https://doi.org/10.1038/ismej.2017.119

Cárdenas, P., & Moore, J. A. (2019). First records of *Geodia* demosponges from the New England seamounts, an opportunity to test the use of DNA mini-barcodes on museum specimens. *Marine Biodiversity*, *49*, 163–174. https://doi.org/10.1007/s12526-017-0775-3

Cárdenas, P., Rapp, H. T., Klitgaard, A. B., Best, M., Thollesson, M., & Tendal, O. S. (2013). Taxonomy, biogeography and DNA barcodes of *Geodia* species (Porifera, Demospongiae, Tetractinellida) in the Atlantic boreo-arctic region. *Zoological Journal of the Linnean Society*, *169*, 251–311. https://doi.org/10.1111/zoj.12056

Cárdenas, P., Rapp, H. T., Schander, C., & Tendal, O. S. (2010). Molecular taxonomy and phylogeny of the Geodiidae (Porifera, Demospongiae, Astrophorida)–combining phylogenetic and Linnaean classification. *Zoologica Scripta*, *39*, 89–106. https://doi.org/10.1111/j.1463-6409.2009.00402.x

Corriero, G., Gadaleta, F., & Bavestrello, G. (2015). A new Mediterranean species of *Tethya* (Porifera: Tethyida: Demospongiae). *Italian Journal of Zoology*, *82*, 535–543. https://doi.org/10.1080/11250003.2015.1077278

Cruz-Barraza, J. A., Vega, C., Ávila, E., & Vázquez-Maldonado, L. E. (2017). Integrative taxonomy reveals the first record and a new species for the previously monotypic genus *Tethytimea* (Tethyida: Tethyidae) in the Gulf of Mexico. *Zootaxa*, *4226*, zootaxa.4226.1.6. https://doi.org/10.11646/zootaxa.4226.1.6

Darriba, D., Taboada, G. L., Doallo, R., & Posada, D. (2012). jModelTest 2: More models, new heuristics and parallel computing.*Nature Methods*, *9*, 772. https://doi.org/10.1038/nmeth.2109

De Cáceres, M., & Legendre, P. (2009). Associations between species and groups of sites: Indices and statistical inference. *Ecology*, *90*, 3566–3574. https://doi.org/10.1890/08-1823.1

de Laubenfels, M. W. (1936). A comparison of the shallow-water sponges near the Pacific end of the Panama Canal with those at the Caribbean end. *Proceedings of the United States National Museum*, *83*, 441–466. https://doi.org/10.5479/si.00963801.83-2993.441

de Laubenfels, M. W., & Hindle, D. E. (1950). The Porifera of the Bermuda archipelago. *The Transactions of the Zoological Society of London*, *27*, 1–154. https://doi.org/10.1111/j.1096-3642.1950.tb00227.x

de Oliveira, B. F. R., Freitas-Silva, J., Sánchez-Robinet, C., & Laport, M. S. (2020). Transmission of the sponge microbiome: Moving towards a unified model. *Environmental Microbiology Reports*, *12*, 619–638. https://doi.org/10.1111/1758-2229.12896

Dendy, A. (1916). Report on the non-Calcareous Sponges collected by Mr. James Hornell at Okhamandal in Kattiawar in 1905-6. Report to the Government of Baroda on the Marine Zoology of Okhamandal in Kattiawar. *Pls. I–IV*, *2*, 93–146.

Derkarabetian, S., Benavides, L. R., & Giribet, G. (2019). Sequence capture phylogenomics of historical ethanol-preserved museum specimens: Unlocking the rest of the vault. *Molecular Ecology Resources*, *19*, 1531–1544. https://doi.org/10.1111/1755-0998.13072

Desqueyroux-Fáundez, R., & Van Soest, R. W. M. (1997). Shallow water Demosponges of the Galápagos Islands.

Revue Suisse de Zoologie, *104*, 379–467. https://doi.org/10.5962/bhl.part.80003

de Voogd, N. J., Alvarez, B., Boury-Esnault, N., Cárdenas, P., Díaz, M.-C., Dohrmann, M., Downey, R., Goodwin, C., Hajdu, E., Hooper, J. N. A., Kelly, M., Klautau, M., Lim, S. C., Manconi, R., Morrow, C., Pinheiro, U., Pisera, A. B., Ríos, P., Rützler, K., … W. M., Xavier, J. (2024). World Porifera Database. Retrieved from https://www.marinespecies.org/porifera on 2024-04-02. https://doi.org/10.14284/359

Díez-Vives, C., & Riesgo, A. (2024). High compositional and functional similarity in the microbiome of deep-sea sponges. *The ISME Journal*, *18*, wrad030. https://doi.org/10.1093/ismejo/wrad030

Díez-Vives, C., Taboada, S., Leiva, C., Busch, K., Hentschel, U., & Riesgo, A. (2020). On the way to specificity - Microbiome reflects sponge genetic cluster primarily in highly structured populations. *Molecular Ecology*, *29*, 4412–4427. https://doi.org/10.1111/mec.15635

Dohrmann, M., Kelley, C., Kelly, M., Pisera, A., Hooper, J. N. A., & Reiswig, H. M. (2017). An integrative systematic framework helps to reconstruct skeletal evolution of glass sponges (Porifera, Hexactinellida). *Frontiers in Zoology*, *14*, 18. https://doi.org/10.1186/s12983-017-0191-3

Duchassaing de Fonbressin, P., & Michelotti, G. (1864). Spongiaires de la mer Caraibe. Natuurkundige Verhandelingen van de Hollandsche Maatschappij Der Wetenschappen Te Haarlem. 21(2), 1–124. pls I–XXV.

Duran, S., & Rützler, K. (2006). Ecological speciation in a Caribbean marine sponge. *Molecular Phylogenetics and Evolution*, *40*, 292–297. https://doi.org/10.1016/j.ympev.2006.02.018

Easson, C. G., Chaves-Fonnegra, A., Thacker, R. W., & Lopez, J. V. (2020). Host population genetics and biogeography structure the microbiome of the sponge *Cliona delitrix*. *Ecology and Evolution*, *10*, 2007–2020. https://doi.org/10.1002/ece3.6033

Ebert, D. (2013). The epidemiology and evolution of symbionts with mixed-mode transmission. *Annual Review of Ecology, Evolution, and Systematics*, *44*, 623–643. https://doi.org/10.1146/annurev-ecolsys-032513-100555

Ellwanger, K., & Nickel, M. (2006). Neuroactive substances specifically modulate rhythmic body contractions in the nerveless metazoan *Tethya wilhelma* (Demospongiae, Porifera). *Frontiers in Zoology*, *3*, 7. https://doi.org/10.1186/1742-9994-3-7

Fan, L., Reynolds, D., Liu, M., Stark, M., Kjelleberg, S., Webster, N. S., & Thomas, T. (2012). Functional equivalence and evolutionary convergence in complex communities of microbial sponge symbionts. *Proceedings of the National Academy of Sciences of the United States of America*, *109*, E1878–E1887. https://doi.org/10.1073/pnas.1203287109

Folmer, O., Black, M., Hoeh, W., Lutz, R., & Vrijenhoek, R. (1994). DNA primers for amplification of mitochondrial cytochrome *c* oxidase subunit I from diverse metazoan invertebrates. *Molecular Marine Biology and Biotechnology*, *3*, 294–299.

Gaino, E., Burlando, B., Buffa, P., & Sarà, M. (1987). Ultrastructural study of the mature egg of *Tethya citrina* Sarà and Melone (Porifera, Demospongiae). *Gamete Research*, *16*, 259–265. https://doi.org/10.1002/mrd.1120160308

Gaino, E., Liaci, L. S., Sciscioli, M., & Corriero, G. (2006). Investigation of the budding process in *Tethya citrina* and *Tethya aurantium* (Porifera, Demospongiae). *Zoomorphology*, *125*, 87–97. https://doi.org/10.1007/s00435-006-0015-z

Gaino, E., & Sarà, M. (1994). An ultrastructural comparative study of the eggs of two species of *Tethya* (Porifera, Demospongiae). *Invertebrate Reproduction & Development*, *26*, 99–106. https://doi.org/10.1080/07924259.1994.9672406

Griffiths, S. M., Antwis, R. E., Lenzi, L., Lucaci, A., Behringer, D. C., Butler, M. J., & Preziosi, R. F. (2019). Host genetics and geography influence microbiome composition in the sponge *Ircinia campana*. *The Journal of Animal Ecology*, *88*, 1684–1695. https://doi.org/10.1111/1365-2656.13065

Hajdu, E., Desqueyroux-Faúndez, R., Carvalho, M. D. S., Lôbo-Hajdu, G., & Willenz, P. (2013). Twelve new Demospongiae (Porifera) from Chilean Fjords, with remarks upon sponge-derived biogeographic compartments in the SE Pacific. *Zootaxa*, *3744*, 1–64. https://doi.org/10.11646/zootaxa.3744.1.1

Heim, I., & Nickel, M. (2010). Description and molecular phylogeny of *Tethya leysae* sp. *nov. Zootaxa*, *21*, 1–21.

Heim, I., Nickel, M., & Brümmer, F. (2007). Phylogeny of the genus *Tethya* (Tethyidae: Hadromerida: Porifera): Molecular and morphological aspects. *Journal of the Marine Biological Association of the United Kingdom*, *87*, 1615–1627. https://doi.org/10.1017/S0025315407058419

Heim, I., Nickel, M., Picton, B., & Brümmer, F. (2007). Description and molecular phylogeny of *Tethya hibernica* sp. nov. (Porifera, Demospongiae) from Northern Ireland with remarks on the European species of the genus *Tethya*. *Zootaxa*, *1595*, 15. https://doi.org/10.11646/zootaxa.1595.1.1

Hentschel, U., Usher, K. M., & Taylor, M. W. (2006). Marine sponges as microbial fermenters. *FEMS Microbiology Ecology*, *55*, 167–177. https://doi.org/10.1111/j.1574-6941.2005.00046.x

Hooper, J. N. A., & Wiedenmayer, F. (1994). Porifera. In A. Wells (Ed.), *Zoological catalogue of Australia* (pp. 1–620). CSIRO Publishing.

Idan, T., Shefer, S., Feldstein, T., Yahel, R., Huchon, D., & Ilan, M. (2018). Shedding light on an East-Mediterranean mesophotic sponge ground community and the regional sponge fauna. *Mediterranean Marine Science*, *19*, 84–106. https://doi.org/10.12681/mms.13853

Katoh, K., & Standley, D. M. (2013). MAFFT Multiple Sequence Alignment Software Version 7: Improvements in performance and usability. *Molecular Biology and Evolution*, *30*, 772–780. https://doi.org/10.1093/molbev/mst010

Kozich, J. J., Westcott, S. L., Baxter, N. T., Highlander, S. K., & Schloss, P. D. (2013). Development of a dual-index sequencing strategy and curation pipeline for analyzing amplicon sequence data on the MiSeq Illumina sequencing platform. *Applied and Environmental Microbiology*, *79*, 5112–5120. https://doi.org/10.1128/AEM.01043-13

Lamarck, J.-B. P. (1815). *Suite des polypiers empâtés* (pp. 1, 69–80, 162–168, 331–340). Mémoires Du Muséum d'Histoire Naturelle. (Original work published 1814)

Laubenfels, M. W. (1932). The marine and fresh-water sponges of California. *Proceedings of the United States National Museum*, *81*, 1–140. https://doi.org/10.5479/si.00963801.81-2927.1

Liaaen-Jensen, S., Renstrøm, B., Ramdahl, T., Hallenstvet, M., & Bergquist, P. (1982). Carotenoids of marine sponges. *Biochemical Systematics and Ecology*, *10*, 167–174. https://doi.org/10.1016/0305-1978(82)90024-2

Łukowiak, M. (2016). Fossil and modern sponge fauna of southern Australia and adjacent regions compared: Interpretation, evolutionary and biogeographic significance of the late Eocene 'soft' sponges. *Contributions to Zoology*, *85*, 13–35. https://doi.org/10.1163/18759866-08501002

Mácola, R., & Menegola, C. (2018). On the Tethyida (Porifera, Demospongiae) from Bahia State, northeast Brazil, with descriptions of two new species, taxonomic appointments and new records. *Zootaxa*, *4433*, 290–304. https://doi.org/10.11646/zootaxa.4433.2.3

Madden, T. (2002). The BLAST sequence analysis tool. In J. McEntyre & J. Ostell (Eds.), *The NCBI Handbook*. National Center for Biotechnology Information (US). Bethesda (MD): National Center for Biotechnology Information (US). Retrieved from https://www.ncbi.nlm.nih.gov/books/NBK21097/

Moitinho-Silva, L., Nielsen, S., Amir, A., Gonzalez, A., Ackermann, G. L., Cerrano, C., Astudillo-Garcia, C., Easson, C., Sipkema, D., Liu, F., Steinert, G., Kotoulas, G., McCormack, G. P., Feng, G., Bell, J. J., Vicente, J., Björk, J. R., Montoya, J. M., Olson, J. B., … Thomas, T. (2017). The sponge microbiome project. *GigaScience*, *6*, 1–7. https://doi.org/10.1093/gigascience/gix077

Moitinho-Silva, L., Steinert, G., Nielsen, S., Hardoim, C. C. P., Wu, Y.-C., McCormack, G. P., López-Legentil, S., Marchant, R., Webster, N., Thomas, T., & Hentschel, U. (2017). Predicting the HMA-LMA status in marine sponges by machine learning. *Frontiers in Microbiology*, *8*, 752. https://doi.org/10.3389/fmicb.2017.00752

Morrow, C., & Cárdenas, P. (2015). Proposal for a revised classification of the Demospongiae (Porifera). *Frontiers in Zoology*, *12*(1), *1*–7. https://doi.org/10.1186/s12983-015-0099-8

Morrow, C. C., Picton, B. E., Erpenbeck, D., Boury-Esnault, N., Maggs, C. A., & Allcock, A. L. (2012). Congruence between nuclear and mitochondrial genes in Demospongiae: A new hypothesis for relationships within the G4 clade (Porifera: Demospongiae). *Molecular Phylogenetics and Evolution*, *62*, 174–190. https://doi.org/10.1016/j.ympev.2011.09.016

Nickel, M., Bullinger, E., & Beckmann, F. (2006). Functional morphology of *Tethya* species (Porifera): 2. Three-dimensional morphometrics on spicules and skeleton superstructures of *T. minuta*. *Zoomorphology*, *125*, 225–239. https://doi.org/10.1007/s00435-006-0022-0

O'Brien, P. A., Webster, N. S., Miller, D. J., & Bourne, D. G. (2019). Host-microbe coevolution: Applying evidence from model systems to complex marine invertebrate holobionts. *mBio*, *10*, 1–14. https://doi.org/10.1128/MBIO.02241-18

Oksanen, J., Blanchet, F. G., Friendly, M., Kindt, R., Legendre, P., McGlinn, D., Minchin, P. R., O'Hara, R. B., Simpson, G. L., Solymos, P., Henry, M., Stevens, H., & Szoecs, E., Wagner, H. (2018). Vegan: Community ecology package. Ordination methods, diversity analysis and other functions for community and vegetation ecologists, Version 2.5-1.

Pallas, P. S. (1766). Elenchus Zoophytorum Sistens Generum Adumbrationes Generaliores et Specierum Cognitarum Succintas Descriptiones, cum Selectis Auctorum Synonymis. Hagæ Comitum: Apud Franciscum Varrentrapp. Retrieved from http://archive.org/details/elenchuszoophyto00pall

Pankey, M. S., Plachetzki, D. C., Macartney, K. J., Gastaldi, M., Slattery, M., Gochfeld, D. J., & Lesser, M. P. (2022). Cophylogeny and convergence shape holobiont evolution in sponge–microbe symbioses. *Nature Ecology & Evolution*, *6*, 750–762. https://doi.org/10.1038/s41559-022-01712-3

Parada, A. E., Needham, D. M., & Fuhrman, J. A. (2016). Every base matters: Assessing small subunit rRNA primers for marine microbiomes with mock communities, time series and global field samples. *Environmental Microbiology*, *18*, 1403–1414. https://doi.org/10.1111/1462-2920.13023

Parks, D. H., Chuvochina, M., Waite, D. W., Rinke, C., Skarshewski, A., Chaumeil, P. A., & Hugenholtz, P. (2018). A standardized bacterial taxonomy based on genome phylogeny substantially revises the tree of life. *Nature Biotechnology*, *36*, 996–1004. https://doi.org/10.1038/nbt.4229

Pita, L., Rix, L., Slaby, B. M., Franke, A., & Hentschel, U. (2018). The sponge holobiont in a changing ocean: From microbes to ecosystems. *Microbiome*, *6*, 46. https://doi.org/10.1186/s40168-018-0428-1

Plese, B., Kenny, N. J., Rossi, M. E., Cárdenas, P., Schuster, A., Taboada, S., Koutsouveli, V., & Riesgo, A. (2021). Mitochondrial evolution in the Demospongiae (Porifera): Phylogeny, divergence time, and genome biology. *Molecular Phylogenetics and Evolution*, *155*, 107011. https://doi.org/10.1016/j.ympev.2020.107011

Reveillaud, J., Allewaert, C., Pérez, T., Vacelet, J., Banaigs, B., & Vanreusel, A. (2012). Relevance of an integrative approach for taxonomic revision in sponge taxa: Case study of the shallow-water Atlanto-Mediterranean *Hexadella* species (Porifera: Ianthellidae: Verongida). *Invertebrate Systematics*, *26*, 230–248. https://doi.org/10.1071/IS11044

Ribeiro, S. M., & Muricy, G. (2004). Four new sympatric species of *Tethya* (Demospongiae: Hadromerida) from Abrolhos Archipelago (Bahia State, Brazil). *Zootaxa*, *557*, 1–16. https://doi.org/10.11646/zootaxa.557.1.1

Ribeiro, S. M., & Muricy, G. (2011). Taxonomic revision of Brazilian *Tethya* (Porifera: Hadromerida) with description of four new species. *Journal of the Marine Biological Association of the United Kingdom*, *91*, 1511–1528. https://doi.org/10.1017/S0025315411000038

Riesgo, A., Cavalcanti, F. F., Kenny, N. J., Ríos, P., Cristobo, J., & Lanna, E. (2018). Integrative systematics of clathrinid sponges: Morphological, reproductive and phylogenetic characterisation of a new species of *Leucetta* from Antarctica (Porifera, Calcarea, Calcinea) with notes on the occurrence of flagellated sperm. *Invertebrate Systematics*, *32*, 827–841. https://doi.org/10.1071/IS17033

Riesgo, A., Pérez-Portela, R., Pita, L., Blasco, G., Erwin, P. M., & López-Legentil, S. (2016). Population structure and connectivity in the Mediterranean sponge *Ircinia fasciculata* are affected by mass mortalities and hybridization. *Heredity*, *117*, 427–439. https://doi.org/10.1038/hdy.2016.41

Ruiz, C., Ivanišević, J., Chevaldonné, P., Ereskovsky, A. V., Boury-Esnault, N., Vacelet, J., Thomas, O. P., & Pérez, T. (2015). Integrative taxonomic description of *Plakina kanaky,* a new polychromatic sponge species from New Caledonia (Porifera: Homoscleromorpha). *Marine Ecology*, *36*, 1129–1143. https://doi.org/10.1111/maec.12209

Samaai, T., & Gibbons, M. J. (2005). Demospongiae taxonomy and biodiversity of the Benguela region on the west coast of South Africa. *African Natural History, 1*, 1–96.

Sarà, M. (1987). A study on the genus *Tethya* (Porifera: Demospongiae) and new perspectives in sponge systematics. In J. Vacelet & N. Boury-Esnault (Eds.), *Taxonomy of Porifera* (Vol. G13, pp. 205–225). NATO ASI Series. Edited Springer-Verlag.

Sarà, M. (1990). Divergence between the sympatric species *Tethya aurantium* and *Tethya citrina* and speciation in sponges. In K. Rützler (Ed.), *New perspectives in sponge biology* (pp. 338–343). Smithsonian Institution Press.

Sarà, M. (1994). A rearrangement of the family Tethyidae (Porifera Hadromerida) with establishment of new genera and description of two new species. *Zoological Journal of the Linnean Society*, *110*, 355–371. https://doi.org/10.1006/zjls.1994.1016

Sarà, M. (2002). Family Tethyidae Gray, 1848. Systema Porifera *(1906),* 245–265. https://doi.org/10.1007/978-1-4615-0747-5_26

Sarà, M., & Bavestrello, G. (1995). *Tethya omanensis*, a remarkable new species from an Oman cave (Porifera, Demospongiae). *Bolletino di Zoologia*, *62*, 23–27. https://doi.org/10.1080/11250009509356046

Sarà, M., & Bavestrello, G. (1998). Two new species of *Tethya* (Porifera, Demospongiae) from the Canary and Cape Verde Islands. *Italian Journal of Zoology*, *65*, 371–376. https://doi.org/10.1080/11250009809386776

Sarà, M., Bavestrello, G., & Calcinai, B. (2000). New *Tethya* species (Porifera, Demospongiae) from the Pacific area. *Zoosystema*, *22*, 345–354.

Sarà, M., Bavestrello, G., & Mensi, P. (1992). Redescription of *Tethya norvegica* Bowerbank (Porifera, Demospongiae), with remarks on the genus Tethya in the North East Atlantic. *Zoologica Scripta*, *21*, 211–216. https://doi.org/10.1111/j.1463-6409.1992.tb00323.x

Sarà, M., & Burlando, B. (1994). Phylogenetic reconstruction and evolutionary hypotheses in the family Tethyidae (Demospongiae). In R. W. M. van Soest, T. M. G. van Kempen, & J.-C. Braekman (Eds.), *Sponges in time and space. Biology, chemistry, paleontology. Proceedings of the 4th International Porifera Congress* (pp. 111–116). A.A. Balkema.

Sarà, M., & Gaino, E. (1987). Interspecific variation in arrangement and morphology of micrasters of *Tethya* species (Porifera, Demospongiae). *Zoomorphology*, *107*, 313–317. https://doi.org/10.1007/BF00312177

Sarà, M., Gómez, P., & Sarà, A. (2001). East Pacific Mexican *Tethya* (Porifera: Demospongiae) with descriptions of five new species. *Proceedings of the Biological Society of Washington*, *114*, 794–821.

Sarà, M., & Melone, N. (1965). Una nuova specie del genere *Tethya*, *Tethya citrina* sp. n. dal Mediterraneo (Porifera Demospongiae). *Atti Della Società Peloritana Di Scienze Fisiche Matematiche e Naturali*, *11*(Supple), 123–138, pls I. II.

Sarà, M., & Sarà, A. (2002). Three remarkable new genera of Tethyidae (Porifera, Demospongiae) from Australia. *Italian Journal of Zoology*, *69*, 163–173. https://doi.org/10.1080/11250000209356455

Sarà, M., & Sarà, A. (2004). A revision of Australian and New Zealand *Tethya* (Porifera: Demospongiae) with a preliminary analysis of species-groupings. *Invertebrate Systematics*, *18*, 117–156. https://doi.org/10.1071/IS03008

Sarà, M., Sarà, A., Nickel, M., & Brümmer, F. (2001). Three new species of *Tethya* (Porifera: Demospongiae) from German Aquaria. *Stuttgarter Beiträge Zur Naturkunde Serie A (Biologie)*, *631*, 1–15.

Schmidt, O. (1862). *Die Spongien des adriatischen Meeres* (pp. i–viii, 1–88, pls. 1–7). Wilhelm Engelmann.

Schmidt, O. (1870). *Grundzüge einer Spongien-Fauna des Atlantischengbietes*. Leipzig.

Schmitt, S., Angermeier, H., Schiller, R., Lindquist, N., & Hentschel, U. (2008). Molecular microbial diversity survey of sponge reproductive stages and mechanistic insights into vertical transmission of microbial symbionts. *Applied and Environmental Microbiology*, *74*, 7694–7708. https://doi.org/10.1128/AEM.00878-08

Schneider, C. A., Rasband, W. S., & Eliceiri, K. W. (2012). NIH Image to ImageJ: 25 years of image analysis. *Nature Methods*, *9*, 671–675. https://doi.org/10.1038/nmeth.2089

Schöttner, S., Hoffmann, F., Cárdenas, P., Rapp, H. T., Boetius, A., & Ramette, A. (2013). Relationships between host phylogeny, host type and bacterial community diversity in cold-water coral reef sponges. *Public Library of Science One*, *8*, e55505. https://doi.org/10.1371/journal.pone.0055505

Sciscioli, M., Lepore, E., Mastrodonato, M., Scalera Liaci, L., & Gaino, E. (2002). Ultrastructural study of the mature oocyte of *Tethya aurantium* (Porifera: Demospongiae). *Cahiers de Biologie Marine*, *43*, 1–8.

Selenka, E. (1879). Ueber einen Kieselschwamm von achtstrahligen Bau, und über Entwicklung der Schwammknospen. *Zeitschrift Für Wissenschaftliche Zoologie*, *33*, 467–476.

Shaffer, M. R., Luter, H. M., Webster, N. S., Abdul Wahab, M. A., & Bell, J. J. (2020). Evidence for genetic structuring and limited dispersal ability in the Great Barrier Reef sponge Carteriospongia foliascens. *Coral Reefs*, *39*, 39–46. https://doi.org/10.1007/s00338-019-01876-8

Shih, J. L., & Popp, B. N. (2020). Assessment of an invasive tropical sponge on coral reefs in Hawaii. *Pacific Science*. *74*, 175–187. https://doi.org/10.2984/74.2.7

Sim-Smith, C., Hickman, C., Jr., & Kelly, M. (2021). New shallow-water sponges (Porifera) from the Galápagos Islands. *Zootaxa*, *5012*, 1–71. https://doi.org/10.11646/zootaxa.5012.1.1

Sipkema, D., & Blanch, H. W. (2010). Spatial distribution of bacteria associated with the marine sponge *Tethya californiana*. *Marine Biology*, *157*, 627–638. https://doi.org/10.1007/s00227-009-1347-2

Sipkema, D., de Caralt, S., Morillo, J. A., Al-Soud, W. A., Sørensen, S. J., Smidt, H., & Uriz, M. J. (2015). Similar sponge-associated bacteria can be acquired via both vertical and horizontal transmission. *Environmental Microbiology*, *17*, 3807–3821. https://doi.org/10.1111/1462-2920.12827

Sollas, W. J. (1885). A classification of the sponges. *Annals and Magazine of Natural History*, *16*(95), 395. https://doi.org/10.1080/00222938509459901

Sollas, W. J. (1888). Report on the Tetractinellida collected by H.M.S. Challenger, during the years 1873–1876. Report on the Scientific Results of the Voyage of H.M.S. Challenger during the Years 1873–76. *Part 63*, *25*, 1–458.

Sorokin, S. J., Ekins, M. G., Yang, Q., & Cárdenas, P. (2019). A new deep-water *Tethya* (Porifera, Tethyida, Tethyidae) from the Great Australian Bight and an updated Tethyida phylogeny. *European Journal of Taxonomy*, *2019*, 1–26. https://doi.org/10.5852/ejt.2019.529

Srivathsan, A., Lee, L., Katoh, K., Hartop, E., Narayanan Kutty, S., Wong, J., Yeo, D., & Meier, R. (2021). MinION barcodes: Biodiversity discovery and identification by

everyone, for everyone. BioRxiv, 2021.03.09.434692. Retrieved from https://doi.org/10.1101/2021.03.09.434692

Stamatakis, A. (2014). RAxML version 8: A tool for phylogenetic analysis and post-analysis of large phylogenies. *Bioinformatics*, *30*, 1312–1313. https://doi.org/10.1093/bioinformatics/btu033

STRI Research Portal Research Data Portal 2023. (2023). *Tethya aurantium*. Smithsonian Tropical Research Institute (*STRI*). Retrieved May 9 from https://panamabiota.org/stri/checklists/checklist.php?clid=35&pid=17

Tanaka, Y., & Yamamoto, A. (1984). The structure of a new carotenoid Tethyanine in sea sponge *Tethya amamensis*. *Nippon Suisan Gakkaishi*, *50*, 1787–1787. https://doi.org/10.2331/suisan.50.1787

Tanaka, Y., Yamamoto, A., & Katayama, T. (1982). Two natural 7-cis aromatic carotenoids from sea sponge *Tethya amamensis*. *Bulletin of the Japanese Society of Scientific Fisheries*, *48*, 1651–1655.

Taylor, J. A., Palladino, G., Wemheuer, B., Steinert, G., Sipkema, D., Williams, T. J., & Thomas, T. (2021). Phylogeny resolved, metabolism revealed: Functional radiation within a widespread and divergent clade of sponge symbionts. *The ISME Journal*, *15*, 503–519. https://doi.org/10.1038/s41396-020-00791-z

Thiel, V., Neulinger, S. C., Staufenberger, T., Schmaljohann, R., & Imhoff, J. F. (2007). Spatial distribution of sponge-associated bacteria in the Mediterranean sponge *Tethya aurantium*. *FEMS Microbiology Ecology*, *59*, 47–63. https://doi.org/10.1111/j.1574-6941.2006.00217.x

Thomas, T., Moitinho-Silva, L., Lurgi, M., Björk, J. R., Easson, C., Astudillo-García, C., Olson, J. B., Erwin, P. M., López-Legentil, S., Luter, H., Chaves-Fonnegra, A., Costa, R., Schupp, P. J., Steindler, L., Erpenbeck, D., Gilbert, J., Knight, R., Ackermann, G., Victor Lopez, J., … Webster, N. S. (2016). Diversity, structure and convergent evolution of the global sponge microbiome. *Nature Communications*, *7*, 11870. https://doi.org/10.1038/ncomms11870

Topsent, E. (1906). Eponges recueillies par M. Ch. Gravier dans la Mer Rouge. *Bulletin Du Muséum National D'Histoire Naturelle*, *12*, 557–570.

Vacelet, J., & Donadey, C. (1977). Electron microscope study of the association between some sponges and bacteria. *Journal of Experimental Marine Biology and Ecology*, *30*, 301–314. https://doi.org/10.1016/0022-0981(77)90038-7

Van Soest, R. W. M., Boury-Esnault, N., Vacelet, J., Dohrmann, M., Erpenbeck, D., De Voogd, N. J., Santodomingo, N., Vanhoorne, B., Kelly, M., & Hooper, J. N. A. (2012). Global diversity of sponges (Porifera). *Public Library of Science One*, *7*, e35105. https://doi.org/10.1371/journal.pone.0035105

Vrijenhoek, R. C. (2010). Genetics and evolution of deep-sea chemosynthetic bacteria and their invertebrate hosts. In S. Kiel (Ed.), *Topics in geobiology* (pp. 15–49). Springer.

Waterworth, S. C., Jiwaji, M., Kalinski, J. C. J., Parker-Nance, S., & Dorrington, R. A. (2017). A place to call home: An analysis of the bacterial communities in two *Tethya rubra* Samaai and Gibbons 2005 populations in Algoa Bay, South Africa. *Marine Drugs*, *15*, 95. https://doi.org/10.3390/md15040095

Weisz, J. B., Hentschel, U., Lindquist, N., & Martens, C. S. (2007). Linking abundance and diversity of sponge-associated microbial communities to metabolic differences in host sponges. *Marine Biology*, *152*, 475–483. https://doi.org/10.1007/s00227-007-0708-y

Wintermann-Kilian, G., & Kilian, E. F. (1984). Marine sponges of the region of Santa Marta (Colombia) Part II. Homosclerophorida, Choristida, Spirophorida, Hadromerida, Axinellida, Halichondrida, Peocilosclerida. *Studies on Neotropical Fauna and Environment*, *19*, 121–135. https://doi.org/10.1038/s41379-020-0580-6

Wright, E. P. (1881). On a new genus and species of sponge with supposed heteromorphic zooids. *The Transactions of the Royal Irish Academy*, *28*, 13–20.

Yang, Q., Franco, C. M. M., & Zhang, W. (2019). Uncovering the hidden marine sponge microbiome by applying a multi-primer approach. *Scientific Reports*, *9*, 6214. https://doi.org/10.1038/s41598-019-42694-w

Associate Editor: Dr Andrea Waeschenbach